

# New contributions to $b \rightarrow s\gamma$ in the minimal G2HDM\*

Che-Hao Liu (劉哲豪)<sup>1†</sup> Van Que Tran (陳文桂)<sup>2,3‡</sup> Qiaoyi Wen (溫侨毅)<sup>4§</sup>  
 Fanrong Xu (徐繁榮)<sup>4§</sup> Tzu-Chiang Yuan (阮自強)<sup>1#</sup>

<sup>1</sup>Institute of Physics, Academia Sinica, Nangang, Taipei 11529, China

<sup>2</sup>Tsung-Dao Lee Institute & School of Physics and Astronomy, Shanghai Jiao Tong University, Shanghai 200240, China

<sup>3</sup>Phenikaa Institute for Advanced Study, Phenikaa University, Yen Nghia, Ha Dong, Hanoi 100000, Vietnam

<sup>4</sup>Department of Physics, College of Physics & Optoelectronic Engineering, Jinan University, Guangzhou 510632, China

**Abstract:** We study flavor-changing bottom quark radiative decay  $b \rightarrow s\gamma$  induced at the one-loop level within the minimal gauged two-Higgs-doublet model (G2HDM). Among the three new contributions to this rare process in G2HDM, we find that only the charged Higgs  $\mathcal{H}^\pm$  contribution can be constrained by the current global fit data in  $B$ -physics. The other two contributions from complex vectorial dark matter  $\mathcal{W}$  and dark Higgs  $\mathcal{D}$  are not sensitive to the current data. Incorporating theoretical constraints imposed on the scalar potential and electroweak precision data for the oblique parameters, we exclude mass regions  $m_{\mathcal{H}}^\pm \lesssim 250$  GeV and  $m_{\mathcal{D}} \lesssim 100$  GeV at the 95% confidence level.

**Keywords:** flavor physics, two-Higgs-doublet-model, dark matter

**DOI:** 10.1088/1674-1137/add873

**CSTR:** 32044.14.ChinesePhysicsC.49083107

## I. INTRODUCTION

The discovery of a Higgs boson near the vicinity of 125 GeV [1, 2] in 2012 completed the building blocks set up in the Standard Model (SM). Well-known unanswered questions in the SM, such as the neutrino masses for neutrino oscillations, dark matter and dark energy problem for the cosmic energy reserve in standard  $\Lambda$ CDM cosmology, and gauge hierarchy problem concerning the stability of the electroweak scale under quantum fluctuations, must be faced by new physics (NP) beyond the SM (BSM). With the direct search limits of new particles at the Large Hadron Collider (LHC) reaching the multi-teraelectronvolt level, many simple extensions of the SM are either severely constrained or completely ruled out. At this stage, all available experimental data must be scrutinized to explore where NP may still be hiding from us. Thus, indirect probes of NP from loop-induced rare processes provide a unique opportunity in this endeavour. Rare  $B$ -meson decays can play a crucial role as both low- $p_T$  and high- $p_T$  searches at the LHCb and LHC, respectively, which are accumulating more precise

and complementary data for the indirect probes.

In this paper, we focus on the one-loop process  $b \rightarrow s\gamma$  in the minimal gauged two-Higgs-doublet model (G2HDM) advocated by some of us [3, 4]. The original model [5] was motivated by gauging the popular inert two-Higgs-doublet model (I2HDM) [6–11] for scalar dark matter, augmented by an extended gauge-Higgs sector of  $SU(2)_H \times U(1)_X$  with a hidden Higgs doublet and hidden Higgs triplet. Thus, the complete Higgs sector of the original model is quite rich but rather complicated to analyze. Nonetheless, various refinements [12, 13] and collider implications [14–18] were pursued with the same particle content as the original model. As demonstrated in [3, 4, 19, 20], we can exclude the hidden Higgs triplet of the extra  $SU(2)_H$  without jeopardizing the symmetry breaking pattern, and realistic mass spectra can also be achieved for phenomenological studies. The interplay between gravitational wave and dark matter signals [21] and the global structure of the G2HDM gauge group [22] have also been studied without the hidden Higgs triplet. Furthermore, omitting the hidden Higgs triplet significantly simplifies the scalar potential by eliminating six

Received 7 March 2025; Accepted 13 May 2025; Published online 14 May 2025

\* Supported in part by the National Natural Science Foundation of China (19Z103010239, 12350410369 (VQT), U1932104 (FRX)) and the NSTC (111-2112-M-001-035 (TCY))

† E-mail: chehao@gate.sinica.edu.tw

‡ E-mail: vqtran@sjtu.edu.cn

§ E-mail: qywen2016051133@stu2016.jnu.edu.cn

# E-mail: fanrongxu@jnu.edu.cn

# E-mail: tcyuan@phys.sinica.edu.tw

 Content from this work may be used under the terms of the Creative Commons Attribution 3.0 licence. Any further distribution of this work must maintain attribution to the author(s) and the title of the work, journal citation and DOI. Article funded by SCOAP<sup>3</sup> and published under licence by Chinese Physical Society and the Institute of High Energy Physics of the Chinese Academy of Sciences and the Institute of Modern Physics of the Chinese Academy of Sciences and IOP Publishing Ltd

parameters. We will refer this as the minimal G2HDM, or simply G2HDM, in this paper.

Because the two Higgs doublets  $H_1$  and  $H_2$  in I2HDM are lumped into an irreducible representation of the hidden  $SU(2)_H$  in G2HDM, new Yukawa couplings occur between the SM and hidden heavy fermions with inert Higgs doublet  $H_2$ . Both the charged and neutral components of  $H_2$  can couple one SM fermion in one generation and one hidden heavy fermion in another generation. The latter yields a flavor changing neutral current (FCNC) Higgs interaction between one SM fermion and one hidden heavy fermion in different generations. Furthermore, unlike the extra gauge boson  $W^\pm$  in left-right symmetric models [23, 24],  $SU(2)_H$  gauge boson  $W^{(p,m)}$ , one of the dark matter candidates in G2HDM, carries no electric charge and hence does not mix with SM  $W^\pm$ .  $W^{(p,m)}$  also results in an FCNC gauge interaction via a right-handed current formed by one SM fermion and one hidden heavy fermion. All other neutral particles in G2HDM, such as the photon,  $Z$ , SM Higgs and its hidden sibling, and dark photon and dark  $Z$ , couple diagonally in flavors with the SM fermion pairs and heavy hidden fermion pairs. Thus, the naturalness of neutral current interactions proposed by Glashow and Weinberg [25] can be fulfilled in G2HDM with regard to the SM sector. Regarding this, we note the following fine point: In [25], a discrete  $Z_2$  symmetry was imposed by hand in the scalar potential of the general 2HDM to forbid unwanted FCNC Higgs interactions with SM fermions at the tree level. However, G2HDM contains an *accidental*  $h$ -parity [17] in the model to guarantee the absence of SM particles coupling to an odd number of new particles, with the odd  $h$ -parity coming from the hidden sector.

All low energy FCNC processes must then be induced by quantum loops in G2HDM. This motivates our interest in rare  $B$  meson decays, in particular  $b \rightarrow s\gamma$ , in this study. We focus on  $b \rightarrow s\gamma$  as a warm up and reserve the more complicated penguin process  $b \rightarrow sl^+l^-$  with  $l = e$  or  $\mu$  for a future effort. These processes are of significant interest in the  $B$ -physics community. For their detailed studies in the popular 2HDM, see, for example, [26, 27].

The remainder of this paper is organized as follows. In Section II, we provide a succinct review of the minimal G2HDM. The relevant G2HDM interaction Lagrangians for the loop computations are given in Section III, followed by a discussion of the Wilson coefficients that govern the amplitudes of  $b \rightarrow s(\gamma, g)$  in Section IV. Relevant flavor phenomenology including renormalization group running effects is discussed in Section V. In Section VI, after a brief discussion of the scanning methodo-

logy, we present our numerical results. We draw our conclusions in VII. Some analytical formulas are relegated to three appendices. Appendix A gives the detailed expressions of the loop amplitudes entered in the Wilson coefficients, Appendix B lists the Feynman parameterized loop integrals with all internal and external masses retained. Finally, in Appendix C, we discuss the recasting of LHC direct search limits of the squarks in the SUSY model to obtain the limits for the hidden quarks in G2HDM.

## II. MINIMAL G2HDM - A SUCCINCT REVIEW

In this section, we briefly review the minimal G2HDM. The quantum numbers of the matter particles in G2HDM under  $SU(3)_C \times SU(2)_L \times SU(2)_H \times U(1)_Y \times U(1)_X$  are<sup>1)</sup>

Scalars:

$$H = (H_1 \ H_2)^T \sim \left( \mathbf{1}, \mathbf{2}, \mathbf{2}, \frac{1}{2}, \frac{1}{2} \right),$$

$$\Phi_H = (G_H^p \ \Phi_H^0)^T \sim \left( \mathbf{1}, \mathbf{1}, \mathbf{2}, 0, \frac{1}{2} \right).$$

We note that the two  $SU(2)_L$  doublets  $H_1$  and  $H_2$  are grouped together as  $H = (H_1 \ H_2)^T$  to form a doublet of  $SU(2)_H$  with a  $U(1)_X$  charge of  $+1/2$ .

Spin 1/2 Fermions:  
Quarks

$$\begin{aligned} Q_L &= (u_L \ d_L)^T \sim \left( \mathbf{3}, \mathbf{2}, \mathbf{1}, \frac{1}{6}, 0 \right), \\ U_R &= (u_R \ u_R^H)^T \sim \left( \mathbf{3}, \mathbf{1}, \mathbf{2}, \frac{2}{3}, \frac{1}{2} \right), \\ D_R &= (d_R^H \ d_R)^T \sim \left( \mathbf{3}, \mathbf{1}, \mathbf{2}, -\frac{1}{3}, -\frac{1}{2} \right), \\ u_L^H &\sim \left( \mathbf{3}, \mathbf{1}, \mathbf{1}, \frac{2}{3}, 0 \right), \quad d_L^H \sim \left( \mathbf{3}, \mathbf{1}, \mathbf{1}, -\frac{1}{3}, 0 \right). \end{aligned}$$

Although the lepton sector is not relevant in this work, it is shown below for completeness.

Leptons

$$\begin{aligned} L_L &= (v_L \ e_L)^T \sim \left( \mathbf{1}, \mathbf{2}, \mathbf{1}, -\frac{1}{2}, 0 \right), \\ N_R &= (v_R \ v_R^H)^T \sim \left( \mathbf{1}, \mathbf{1}, \mathbf{2}, 0, \frac{1}{2} \right), \\ E_R &= (e_R^H \ e_R)^T \sim \left( \mathbf{1}, \mathbf{1}, \mathbf{2}, -1, -\frac{1}{2} \right), \\ v_L^H &\sim (\mathbf{1}, \mathbf{1}, \mathbf{1}, 0, 0), \quad e_L^H \sim (\mathbf{1}, \mathbf{1}, \mathbf{1}, -1, 0). \end{aligned}$$

1) The last two entries in the tuples are the  $Y$  hypercharge and  $X$  charge of the two  $U(1)$  factors. Note that the  $Q_X$  charges of  $\pm 1$  of the some fields in our earlier works [5, 12–18] had been changed to  $\pm 1/2$  here. This makes the interaction terms for the hidden  $X$  gauge field look similar to those of the  $B$  gauge field associated with the hypercharge. The anomaly cancellation remains intact with these changes.

The most general renormalizable Higgs potential, which is invariant under both  $SU(2)_L \times U(1)_Y$  and  $SU(2)_H \times U(1)_X$ , can be expressed as follows:

$$\begin{aligned} V = & -\mu_H^2 (H^{\alpha i} H_{\alpha i}) - \mu_\Phi^2 \Phi_H^\dagger \Phi_H + \lambda_H (H^{\alpha i} H_{\alpha i})^2 + \lambda_\Phi (\Phi_H^\dagger \Phi_H)^2 \\ & + \frac{1}{2} \lambda'_H \epsilon_{\alpha\beta} \epsilon^{\gamma\delta} (H^{\alpha i} H_{\gamma i}) (H^{\beta j} H_{\delta j}) \\ & + \lambda_{H\Phi} (H^\dagger H) (\Phi_H^\dagger \Phi_H) + \lambda'_{H\Phi} (H^\dagger \Phi_H) (\Phi_H^\dagger H), \end{aligned} \quad (1)$$

where  $(i, j)$  and  $(\alpha, \beta, \gamma, \delta)$  refer to the  $SU(2)_L$  and  $SU(2)_H$  indices, respectively, all of which range from 1 to 2. We denote  $H^{\alpha i} = H_{\alpha i}^*$ ; therefore,  $H^\dagger H = H^{\alpha i} H_{\alpha i}$  and  $(H^\dagger \Phi_H) (\Phi_H^\dagger H) = (H^{\alpha i} \Phi_{H\alpha}) (\Phi_{H\beta}^* H_{\beta i})$ .

To study spontaneous symmetry breaking (SSB) in the model, we parameterize the Higgs fields linearly according to standard lore:

$$H_1 = \begin{pmatrix} G^+ \\ \frac{v+h_{\text{SM}}}{\sqrt{2}} + i \frac{G^0}{\sqrt{2}} \end{pmatrix}, \quad H_2 = \begin{pmatrix} \mathcal{H}^+ \\ \mathcal{H}_2^0 \end{pmatrix}, \quad (2)$$

$$\Phi_H = \begin{pmatrix} G_H^p \\ \frac{v_\Phi + \phi_H}{\sqrt{2}} + i \frac{G_H^0}{\sqrt{2}} \end{pmatrix}, \quad (3)$$

where  $v$  and  $v_\Phi$  are the only non-vanishing vacuum expectation values (VEVs) in the SM doublet  $H_1$  and hidden doublet  $\Phi_H$  fields, respectively;  $v = 246$  GeV is the SM VEV and  $v_\Phi$  is a hidden VEV at the teraelectronvolt scale.  $H_2$  is the inert doublet with  $\langle H_2 \rangle = 0$ . In essence, the scalar sector of the minimal G2HDM is a special tailored 3HDM.

### III. G2HDM INTERACTIONS

In this section, we provide the relevant interaction Lagrangians and other information for the computation of  $b \rightarrow s(\gamma, g)$  at one-loop order in the minimal G2HDM. We will primarily follow the convention in Peskin and Schroeder<sup>1)</sup>.

In addition to introducing the CKM unitary mixing matrix,

$$V_{\text{CKM}} \equiv (U_u^L)^\dagger U_d^L = \begin{pmatrix} V_{ud} & V_{us} & V_{ub} \\ V_{cd} & V_{cs} & V_{cb} \\ V_{td} & V_{ts} & V_{tb} \end{pmatrix}, \quad (4)$$

which diagonalizes the mass matrices of SM quarks, we

must also introduce the following two unitary mixing matrices that diagonalizes the mass matrices of heavy new quarks in G2HDM:

$$V_u^H \equiv (U_u^R)^\dagger U_{u^H}^R, \quad (5)$$

$$V_d^H \equiv (U_d^R)^\dagger U_{d^H}^R. \quad (6)$$

#### A. Photon, gluon, and $W^\pm$ interactions

For the photon, the relevant interaction Lagrangian is

$$\begin{aligned} \mathcal{L}^\gamma \supset & -ie \left( \mathcal{H}^+ \overset{\leftrightarrow}{\partial}_\mu \mathcal{H}^- \right) A^\mu + e \left[ Q_u \sum_{q=u,c,t} (\bar{q} \gamma_\mu q + \bar{q}^H \gamma_\mu q^H) \right. \\ & \left. + Q_d \sum_{q=d,s,b} (\bar{q} \gamma_\mu q + \bar{q}^H \gamma_\mu q^H) \right] A^\mu \\ & + ie \left[ (\partial_\mu W_v^+ - \partial_v W_\mu^+) W^{\mu-} A^\nu - (\partial_\mu W_v^- - \partial_v W_\mu^-) W^{\mu+} A^\nu \right. \\ & \left. + \frac{1}{2} (\partial_\mu A_\nu - \partial_\nu A_\mu) (W^{\mu+} W^{-\nu} - W^{-\mu} W^{+\nu}) \right], \end{aligned} \quad (7)$$

where  $(a \overset{\leftrightarrow}{\partial}_\mu b) \equiv a \partial_\mu b - b \partial_\mu a$ ,  $Q_u = 2/3$ , and  $Q_d = -1/3$ .

For the gluon, we have

$$\mathcal{L}^g \supset g_s \sum_{q=u,d,s,c,b,t} (\bar{q} T^a \gamma_\mu q + \bar{q}^H T^a \gamma_\mu q^H) G_a^\mu, \quad (8)$$

where  $T^a$  denotes the generators of color group  $SU(3)_C$  associated with gluon fields  $G_a^\mu$  for  $a = 1, \dots, 8$ .

The SM charged current interaction for the quarks is

$$\mathcal{L}^W \supset \frac{g}{2\sqrt{2}} \sum_{i,j} \bar{u}_j (V_{\text{CKM}})_{ji} \gamma^\mu (1 - \gamma_5) d_i W_\mu^+ + \text{h.c.} \quad (9)$$

where  $V_{\text{CKM}}$  is defined in (4) with  $i, j$  being the generation indices. Because the effective Lagrangian describing rare FCNC decays  $b \rightarrow s(\gamma, g)$  is given by the chirality flipped transition dipole operators, the chiral  $V-A$  structure of SM interaction (9) implies that the loop amplitudes can enjoy the enhancement by two internal top quark mass insertions, in addition to the mass insertion from either side of the external lines owing to the equation of motion. This is to be compared with similar processes  $t \rightarrow c(\gamma, g)$  in which the SM contribution results from the Hermitian conjugate of (9) and, hence, involves two bottom quark mass insertions instead. This distinctive feature is reflected in the SM branching ratios of

1) M. E. Peskin and D. V. Schroeder, "An Introduction to quantum field theory," Addison-Wesley, 1995, ISBN 978-0-201-50397-5

$b \rightarrow s\gamma$  and  $t \rightarrow c\gamma$ , which are about  $\sim 3 \times 10^{-4}$  [28, 29] and  $\sim 10^{-14}$  [30], respectively.

## B. G2HDM interactions

G2HDM has three new charged (electric charge or dark charge) current interactions mediated by dark Higgs  $\mathcal{D}$ , charged Higgs  $\mathcal{H}^\pm$ , and  $\mathcal{W}^{(p,m)}$  that can produce  $b \rightarrow s(\gamma, g)$  at one-loop order. The first contribution is from dark Higgs  $\mathcal{D}$ , which is a linear combination of two odd  $h$ -parity components  $\mathcal{H}_2^0$  and  $G_H^m$ <sup>1)</sup>

$$\mathcal{D} = \cos \theta_2 \mathcal{H}_2^0 + \sin \theta_2 G_H^m, \quad (10)$$

where  $\theta_2$  is a mixing angle giving by

$$\tan 2\theta_2 = \frac{2vv_\Phi}{v_\Phi^2 - v^2}. \quad (11)$$

The mass of  $\mathcal{D}$  is

$$m_{\mathcal{D}}^2 = \frac{1}{2} \lambda'_{H\Phi} (v^2 + v_\Phi^2). \quad (12)$$

The relevant interaction Lagrangian for dark boson  $\mathcal{D}$  interacts with SM down-type quarks  $d_i$  and new heavy down-type quarks  $d_j^H$  in G2HDM is given by

$$\mathcal{L}^{\mathcal{D}} \supset \sum_{i,j} \overline{d_j^H} \left[ (S_d^{\mathcal{D}})_{ji} + (P_d^{\mathcal{D}})_{ji} \gamma_5 \right] d_i \mathcal{D}^* + \text{h.c.} \quad (13)$$

where Yukawa couplings matrices  $S_d^{\mathcal{D}}$  and  $P_d^{\mathcal{D}}$  are given by

$$(S_d^{\mathcal{D}})_{ji} = \frac{\sqrt{2}}{2v} \cos \theta_2 (V_d^{H\dagger} M_d)_{ji} + \frac{\sqrt{2}}{2v_\Phi} \sin \theta_2 (M_{d^H} V_d^{H\dagger})_{ji}, \quad (14)$$

$$(P_d^{\mathcal{D}})_{ji} = -\frac{\sqrt{2}}{2v} \cos \theta_2 (V_d^{H\dagger} M_d)_{ji} + \frac{\sqrt{2}}{2v_\Phi} \sin \theta_2 (M_{d^H} V_d^{H\dagger})_{ji}, \quad (15)$$

with  $V_d^H$  defined in (6) and

$$M_d = \text{diag}(m_d, m_s, m_b), \quad (16)$$

$$M_{d^H} = \text{diag}(m_{d^H}, m_{s^H}, m_{b^H}). \quad (17)$$

Note that the ordering of the mass and mixing matrices

1) The other orthogonal combination is  $\tilde{G} = -\sin \theta_2 \mathcal{H}_2^0 + \cos \theta_2 G_H^m$ , which together with its complex conjugate, are the Goldstone bosons absorbed by the longitudinal components of  $\mathcal{W}^{(m,p)}$ .

are important in the Yukawa couplings (14) and (15). Additionally, fixing  $v$ ,  $v_\Phi$ , and  $V_d^H$ , for small (large) mixing angle  $\theta_2$ , these Yukawa couplings are suppressed (enhanced) by down-type quark (heavy quark) mass  $M_d$  ( $M_{d^H}$ ). For  $v_\Phi \gg v$ , the contributions from  $\mathcal{D}$  are expected to be minuscule. Similar small effects from  $\mathcal{D}$  have also been observed in  $t \rightarrow c(\gamma, g)$  [31].

The second contribution to  $b \rightarrow s(\gamma, g)$  is from the dark charged Higgs  $\mathcal{H}^\pm$ , which is quite peculiar in G2HDM compared with another multi-Higgs doublet model because it has odd  $h$ -parity. Thus, the following vertices  $W^\pm \mathcal{H}^\mp \gamma$ ,  $W^\pm \mathcal{H}^\mp Z$ , and  $W^\pm \mathcal{H}^\mp h$  are all nil in the model. The mass of the charged Higgs is given by

$$m_{\mathcal{H}^\pm}^2 = \frac{1}{2} (\lambda'_{H\Phi} v_\Phi^2 - \lambda'_H v^2). \quad (18)$$

The relevant interaction Lagrangian for the charged Higgs exchange is

$$\mathcal{L}^{\mathcal{H}} \supset \sum_{i,j} \overline{u_j^H} \left[ (y_u^{\mathcal{H}})_{ji} (1 - \gamma_5) \right] d_i \mathcal{H}^+ + \text{h.c.} \quad (19)$$

where Yukawa coupling matrix  $y_u^{\mathcal{H}}$  is given by

$$(y_u^{\mathcal{H}})_{ji} = \frac{\sqrt{2}}{2v} (V_u^{H\dagger} M_u V_{CKM})_{ji}, \quad (20)$$

with  $V_{CKM}$  and  $V_u^H$  defined in (4) and (5), respectively, and

$$M_u = \text{diag}(m_u, m_c, m_t). \quad (21)$$

Because Yukawa coupling  $y_u^{\mathcal{H}}$  is proportional to up-type quark mass matrix  $M_u$ , we expect that the charged Higgs contribution to  $b \rightarrow s(\gamma, g)$  from the third generation heavy fermions is more relevant than the  $\mathcal{D}$  contribution. This is to be compared with the charged Higgs contribution to  $t \rightarrow c(\gamma, g)$ , where the corresponding Yukawa coupling  $y_d^{\mathcal{H}} = \sqrt{2}(V_{CKM} M_d V_d^H)/2v$  is proportional to down-type quark mass matrix  $M_d$  and, therefore, has a smaller impact [31].

The third contribution to  $b \rightarrow s(\gamma, g)$  is from the vector dark matter  $\mathcal{W}^{(p,m)}$  assumed to be the lightest  $h$ -parity odd particle in the minimal G2HDM, with mass given by

$$m_{\mathcal{W}} = \frac{1}{2} g_H \sqrt{v^2 + v_\Phi^2}. \quad (22)$$

The relevant interaction Lagrangian for  $\mathcal{W}$  is given by

$$\mathcal{L}^W \supset \frac{g_H}{2\sqrt{2}} \sum_{i,j} \bar{d}_j^H \left[ (V_d^{H\dagger})_{ji} \gamma^\mu (1 + \gamma_5) \right] d_i W_\mu^p + \text{h.c.} \quad (23)$$

Note that the dark matter gauge boson  $\mathcal{W}$  couples to a right-handed current formed by one SM fermion and one hidden heavy fermion. However, from our previous works, we know hidden gauge coupling  $g_H$  is constrained to be small, of order one percent or less; thus, we expect the contribution to processes  $b \rightarrow s(\gamma, g)$  from dark matter  $\mathcal{W}$  to not be significant, too. A similar result was found for  $t \rightarrow c(\gamma, g)$  [31].

Interaction Lagrangians  $\mathcal{L}^D$ ,  $\mathcal{L}^H$ , and  $\mathcal{L}^W$  given by

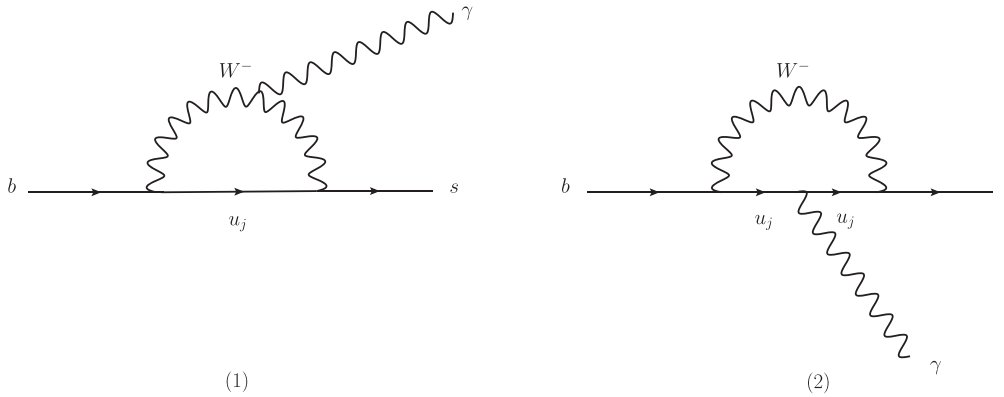


**Fig. 1.** Contributions to  $b \rightarrow s\gamma$  from the SM  $W^\pm$  loop in the unitary gauge.

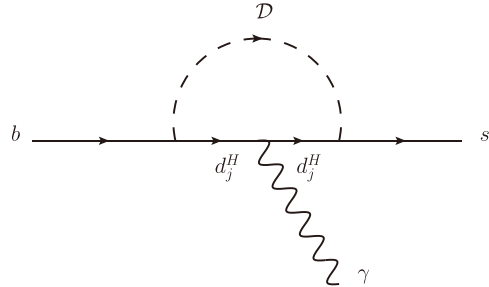


**Fig. 2.** Contribution to  $b \rightarrow s\gamma$  from the  $D$  loop.

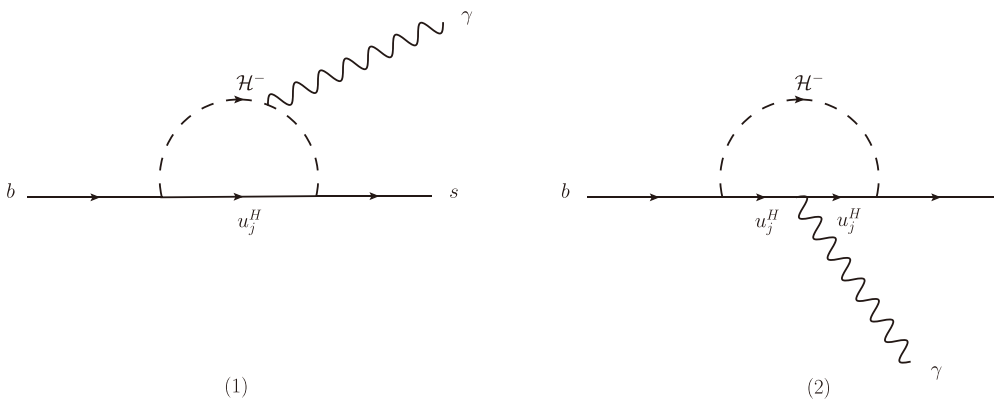


**Fig. 3.** Contributions to  $b \rightarrow s\gamma$  from the  $H^\pm$  loop.

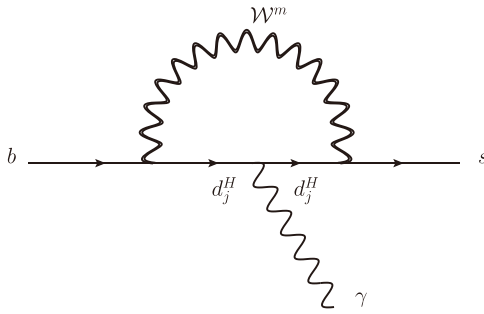


**Fig. 4.** Contribution to  $b \rightarrow s\gamma$  from the  $W^{(p,m)}$  loop in the unitary gauge.

#### IV. WILSON COEFFICIENTS FOR $b \rightarrow s(\gamma, g)$

As mentioned earlier, processes  $b \rightarrow s(\gamma, g)$  can be described by the following effective Lagrangian:

$$\mathcal{L}_{\text{eff}} = -\frac{1}{32\pi^2} e m_b \bar{s} \sigma_{\mu\nu} (A^M + i\gamma_5 A^E) b F^{\mu\nu} + \frac{1}{32\pi^2} g_s m_b \bar{s} \sigma_{\mu\nu} T^a (C^M + i\gamma_5 C^E) b G_a^{\mu\nu}, \quad (24)$$

where  $A^M(C^M)$  and  $A^E(C^E)$  are the transition (chromo)magnetic and (chromo)electric dipole form factors, respectively, and  $F^{\mu\nu}(G_a^{\mu\nu})$  is the electromagnetic (gluon) field strength. Our task is to compute and evaluate these form factors for the on-shell photon at one-loop order from the SM  $W$  boson loop, as well as the three new contributions in the minimal G2HDM, as described in Section III.

The computation is similar to charged lepton flavor violation process  $s l_i \rightarrow l_j \gamma$  presented in [32]; therefore, we can simply recycle our previous formulas. The total contribution for  $b \rightarrow s\gamma$  in minimal G2HDM is given by

$$A^{(M,E)} = A^{(M,E)}(W) + \Delta A^{(M,E)}, \quad (25)$$

where

$$\Delta A^{(M,E)} = A^{(M,E)}(\mathcal{D}) + (A_1^{(M,E)}(\mathcal{H}) + A_2^{(M,E)}(\mathcal{H})) + A^{(M,E)}(\mathcal{W}). \quad (26)$$

SM contributions  $A^{(M,E)}(W)$  and new contributions  $A^{(M,E)}(\tilde{D})$ ,  $A_{1,2}^{(M,E)}(\mathcal{H})$ , and  $A^{(M,E)}(\mathcal{W})$  are given in Appendix A.

Similarly, the total contribution to  $b \rightarrow sg$  is given by

$$C^{(M,E)} = C^{(M,E)}(W) + \Delta C^{(M,E)}, \quad (27)$$

where

$$\Delta C^{(M,E)} = C^{(M,E)}(\mathcal{D}) + C^{(M,E)}(\mathcal{H}) + C^{(M,E)}(\mathcal{W}), \quad (28)$$

with

$$C^{(M,E)}(W) = A_2^{(M,E)}(W)/Q_u, \quad (29)$$

$$C^{(M,E)}(\mathcal{D}) = A^{(M,E)}(\mathcal{D})/Q_d, \quad (30)$$

$$C^{(M,E)}(\mathcal{H}) = A_2^{(M,E)}(\mathcal{H})/Q_u, \quad (31)$$

$$C^{(M,E)}(\mathcal{W}) = A^{(M,E)}(\mathcal{W})/Q_d. \quad (32)$$

In the  $B$ -physics community, processes  $b \rightarrow s(\gamma, g)$  are frequently described by the effective Hamiltonian as [33]

$$\mathcal{H}_{\text{eff}} = -\frac{4G_F}{\sqrt{2}} \frac{e^2}{16\pi^2} V_{tb} V_{ts}^* [C_7(\mu) O_7(\mu) + C'_7(\mu) O'_7(\mu) + C_8(\mu) O_8(\mu) + C'_8(\mu) O'_8(\mu)] + \text{h.c.}, \quad (33)$$

with operators

$$O_7 = \frac{m_b}{e} \bar{s} \sigma_{\mu\nu} P_R b F^{\mu\nu}, \quad O'_7 = \frac{m_b}{e} \bar{s} \sigma_{\mu\nu} P_L b F^{\mu\nu}, \quad (34)$$

$$O_8 = g_s \frac{m_b}{e^2} \bar{s} \sigma_{\mu\nu} T^a P_R b G_a^{\mu\nu}, \quad O'_8 = g_s \frac{m_b}{e^2} \bar{s} \sigma_{\mu\nu} T^a P_L b G_a^{\mu\nu}, \quad (35)$$

where  $P_{L,R} = (1 \mp \gamma_5)/2$  are the chiral projection operators,  $G_F$  is the Fermi constant, and  $C_{7,8}^{(\prime)}(\mu)$  denotes the dimensionless Wilson coefficients at scale  $\mu$ . These Wilson coefficients contain two parts:

$$C_{7,8}^{(\prime)}(\mu) = C_{7,8 \text{ SM}}^{(\prime)}(\mu) + \Delta C_{7,8}^{(\prime)}(\mu). \quad (36)$$

Comparing effective Hamiltonian  $\mathcal{H}_{\text{eff}}$  in (33) with  $(-\mathcal{L}_{\text{eff}})$  in (24), we can read off Wilson coefficients  $C_{7,8}^{(\prime)}(M)$  at high mass scale  $M$  where the heavy particles in G2HDM are integrated out. Explicitly, for the SM  $W$  contribution, we find

$$(C_{7 \text{ SM}}(M), C'_{7 \text{ SM}}(M)) = -\left(\frac{8G_F}{\sqrt{2}}\right)^{-1} (V_{tb} V_{ts}^*)^{-1} \times (A^M(W) + iA^E(W), A^M(W) - iA^E(W)), \quad (37)$$

$$(C_{8\text{SM}}(M), C'_{8\text{SM}}(M)) = + \left( \frac{8G_F}{\sqrt{2}} \right)^{-1} (V_{tb} V_{ts}^*)^{-1} \times (C^M(W) + iC^E(W), C^M(W) - iC^E(W)), \quad (38)$$

and the new contributions from G2HDM:

$$(\Delta C_7(M), \Delta C'_7(M)) = - \left( \frac{8G_F}{\sqrt{2}} \right)^{-1} (V_{tb} V_{ts}^*)^{-1} \times (\Delta A^M + i\Delta A^E, \Delta A^M - i\Delta A^E), \quad (39)$$

$$(\Delta C_8(M), \Delta C'_8(M)) = + \left( \frac{8G_F}{\sqrt{2}} \right)^{-1} (V_{tb} V_{ts}^*)^{-1} \times (\Delta C^M + i\Delta C^E, \Delta C^M - i\Delta C^E), \quad (40)$$

where  $\Delta A^{(M,E)}$  and  $\Delta C^{(M,E)}$  are defined in (26) and (28), respectively.

In practice, we would set high mass scale  $M$  to be the  $W$  boson mass and use QCD renormalization group equations (RGEs) to evolve the Wilson coefficients down to  $\mu = m_b$  to evaluate the hadronic matrix elements for  $b \rightarrow s$  transitions.

## V. FLAVOR PHENOMENOLOGY

Both inclusive and exclusive decays are considered in the following analysis. For the inclusive decay,  $\mathcal{B}(B \rightarrow X_s \gamma)$  can be calculated through the following semi-analytic linearized expression [34]:

$$10^4 \mathcal{B}(\bar{B} \rightarrow X_s \gamma) = (3.40 \pm 0.17) - 8.25 \Delta C_7 - 2.10 \Delta C_8. \quad (41)$$

The unprimed effective coefficients can be evaluated via the RGE evolution

$$\mu \frac{d\vec{C}^{\text{eff}}(\mu)}{d\mu} = \gamma^T \vec{C}^{\text{eff}}(\mu), \quad (42)$$

where the anomalous dimension matrix is defined as  $\gamma = \sum_{n=0}^{\infty} \gamma^n \left( \frac{\alpha_s(\mu)}{4\pi} \right)^{n+1}$  with  $\gamma^n$  of next-to-leading order (NLO) [35, 36] and next-to-next-to-leading order (NNLO) [37–39]. For the effective coefficients [35, 40, 41] at the electroweak scale, here we adopt convention  $C_{7,8}^{\text{eff}} = C_{7,8} + \sum_{j=1}^6 y_j^{(7,8)} C_j$  with  $y_j^{(7)} = (0, 0, -\frac{1}{3}, -\frac{4}{9}, -\frac{20}{3}, -\frac{80}{9})$

and  $y_j^{(8)} = (0, 0, 1, -\frac{1}{6}, 20, -\frac{10}{3})$ . Note that, in the practical calculation, we have neglected NP contributions to four-quark operators  $O_{1,\dots,6}$ . Because new particles in G2HDM should not emerge between  $\mu_W$  and  $\mu_t$ , the primed coefficients  $C_{7,8}^{\text{eff}}$  share the common evolution equations with their chiral-flipped counterparts [42–44].

The branching fraction of exclusive radiative decay  $B \rightarrow V\gamma$  can be generally expressed [45] as

$$\mathcal{B}(B_q \rightarrow V\gamma) = \tau_{B_q} \frac{\alpha_e G_F^2 m_{B_q}^3 m_b^2}{32\pi^4} \left( 1 - \frac{m_V^2}{m_B^2} \right)^3 \times |\lambda_t|^2 (|C_7^{\text{eff}}|^2 + |C'_7|^2) T_1(0), \quad (43)$$

where the final state dependent form factors  $T_1(0)$  are taken from [45] based on a combination with the light-cone sum rule and Lattice QCD. Here,  $V$  denotes a vector meson such as  $\phi$ ,  $K^{*0}$ , and  $K^{*\pm}$ .

In the normalized CP asymmetry for  $B_s \rightarrow V\gamma$ , assuming its parametrization obeying generic time dependent form <sup>1)</sup>, the observables are defined [46] as

$$C_{V\gamma} = \frac{|\mathcal{A}_L|^2 + |\mathcal{A}_R|^2 - |\bar{\mathcal{A}}_R|^2 - |\bar{\mathcal{A}}_L|^2}{|\mathcal{A}_L|^2 + |\bar{\mathcal{A}}_L|^2 + |\mathcal{A}_R|^2 + |\bar{\mathcal{A}}_R|^2}, \\ S_{V\gamma} = 2\Im \left[ \frac{\frac{q}{p}(\bar{\mathcal{A}}_L \mathcal{A}_L^* + \bar{\mathcal{A}}_R \mathcal{A}_R^*)}{|\mathcal{A}_L|^2 + |\bar{\mathcal{A}}_L|^2 + |\mathcal{A}_R|^2 + |\bar{\mathcal{A}}_R|^2} \right], \\ A_{V\gamma}^\Delta = 2\Re \left[ \frac{\frac{q}{p}(\bar{\mathcal{A}}_L \mathcal{A}_L^* + \bar{\mathcal{A}}_R \mathcal{A}_R^*)}{|\mathcal{A}_L|^2 + |\bar{\mathcal{A}}_L|^2 + |\mathcal{A}_R|^2 + |\bar{\mathcal{A}}_R|^2} \right], \quad (44)$$

in terms of amplitudes  $\mathcal{A}_{L(R)} = \mathcal{N} C_7^{(\prime)\text{eff}} T_1(0)$  and  $\bar{\mathcal{A}}_{L(R)} \equiv \mathcal{A}(\bar{B}_s \rightarrow V\gamma_{L(R)})$  with  $\mathcal{N} = \lambda_t \sqrt{\frac{G_F^2 \alpha_e m_B^3}{32\pi^4} \left( 1 - \frac{m_V^2}{m_B^2} \right)^3}$ . In particular,  $\bar{\mathcal{A}}_{L(R)}$  can be derived straightforwardly from  $\mathcal{A}_{L(R)}$  by taking weak phase as conjugated while keeping the strong phase unchanged. The defined ratio is  $\left( \frac{q}{p} \right)_s = \left| \frac{q}{p} \right|_s e^{-i\phi_s}$  and  $\left| \frac{q}{p} \right|_s = 1$  has been utilized to derive Eq. (44) <sup>2)</sup>.

To date, the branching fractions of  $B^{(0,+)} \rightarrow K^{*(0,+)}\gamma$ ,  $B \rightarrow \phi\gamma$ , and CP asymmetry parameters of  $B_s \rightarrow \phi\gamma$  have been measured, which are taken as inputs in the following numerical analysis.

## VI. NUMERICAL ANALYSIS

In this section, we present the numerical results that include the new contributions to Wilson coefficients  $C_7^{(\prime)}$  and  $C_8^{(\prime)}$  and the preferred regions on the model parameter space for data from various low-energy flavor observ-

1) In the parametrization  $\mathcal{A}_{CP}(B_s \rightarrow V\gamma)[t] = \frac{S \sin(\Delta m_s t) - C \cos(\Delta m_s t)}{\cosh(\frac{1}{2}\Delta\Gamma_s t) - H \cosh(\frac{1}{2}\Delta\Gamma_s t)}$ , we adopt the convention  $C_{V\gamma} = C$ ,  $S_{V\gamma} = S$ ,  $A_{V\gamma}^\Delta = H$  in this work.

2) Here we simply adopt the experimental average value  $\phi_s = -0.010 \pm 0.014$  [47] in the following numerical analysis.

ables, as well as the constraints derived from theoretical conditions on the scalar potential and oblique parameters. In this analysis, we assume the new mixing matrices  $V_u^H \equiv V_d^H \equiv V_{\text{CKM}}$  and fix the hidden quark masses as  $m_{s^H} = m_{d^H}$ ,  $m_{b^H} = m_{d^H} + \Delta m_{d^H}$  for down-type quarks and  $m_{c^H} = m_{u^H}$ ,  $m_{t^H} = m_{u^H} + \Delta m_{u^H}$  for up-type quarks.

### A. New contributions to Wilson coefficients

$$C_7^{(\prime)} \text{ and } C_8^{(\prime)}$$

Before we examine the parameter space within the model with respect to observations from low-energy flavor experiments, we determine the relative magnitudes of the new contributions to Wilson coefficients  $\Delta C_7^{(\prime)}$  and  $\Delta C_8^{(\prime)}$ .

**Figure 5** shows the real part of  $\Delta C_7$  and  $\Delta C_8$ . The imaginary parts of  $\Delta C_7^{(\prime)}$  and  $\Delta C_8^{(\prime)}$ , resulting primarily

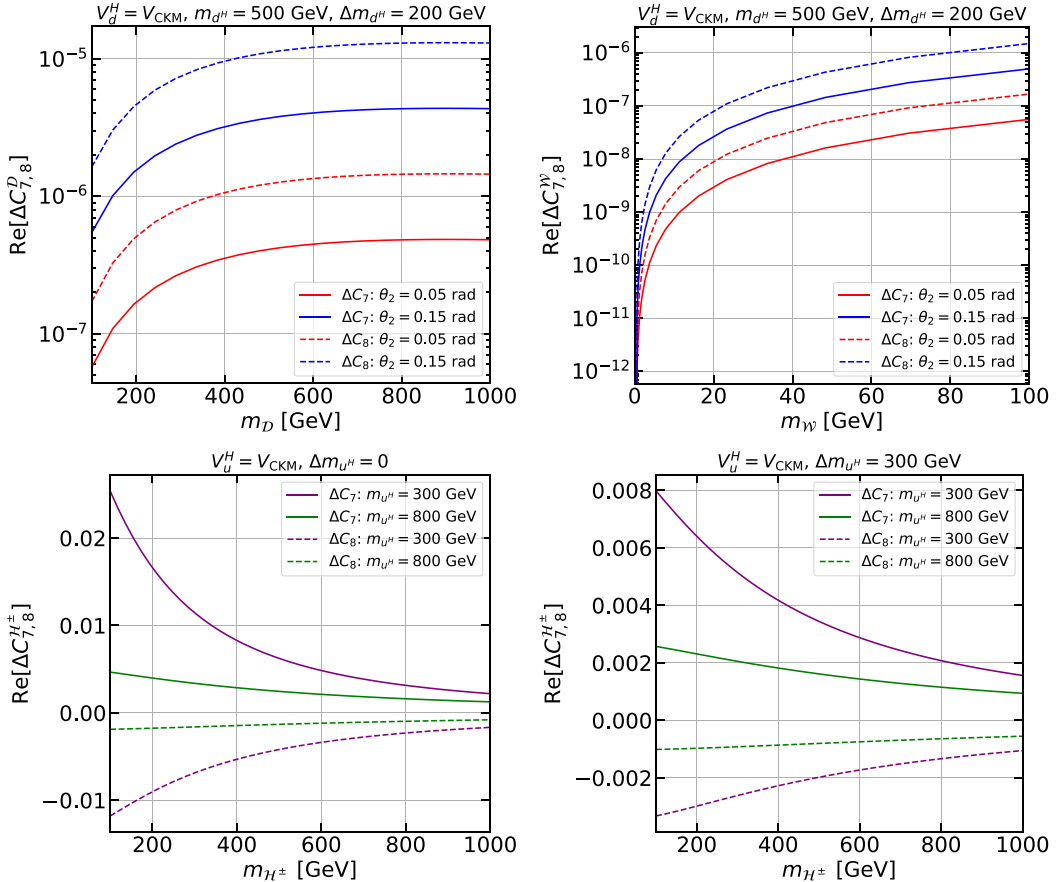


**Fig. 5.** (color online) Real part of the new contributions to Wilson coefficients  $\Delta C_7$  and  $\Delta C_8$ . Top panels: Contribution from the  $\mathcal{D}$  loop as a function of  $m_D$  (left) and from the  $\mathcal{W}$  loop as a function of  $m_W$  (right). We set  $V_d^H = V_{\text{CKM}}$ ,  $m_{d^H} = 500 \text{ GeV}$ , and  $\Delta m_{d^H} = 200 \text{ GeV}$ . The solid (dashed) blue and red lines indicate  $\text{Re}[\Delta C_7]$  ( $\text{Re}[\Delta C_8]$ ) with fixed  $\theta_2 = 0.05 \text{ rad}$  and  $\theta_2 = 0.15 \text{ rad}$ , respectively. Bottom panels: Contribution from the  $\mathcal{H}^\pm$  loop as a function of  $m_{\mathcal{H}^\pm}$ , with  $V_u^H = V_{\text{CKM}}$  and  $\Delta m_{u^H} = 0 \text{ GeV}$  for the left panel, and  $\Delta m_{u^H} = 300 \text{ GeV}$  for the right panel. The solid (dashed) purple and green lines represent  $\text{Re}[\Delta C_7]$  ( $\text{Re}[\Delta C_8]$ ) with fixed  $m_{u^H} = 300 \text{ GeV}$  and  $m_{u^H} = 800 \text{ GeV}$ , respectively.

1) The choice of  $\theta_2$  values adheres to the current constraints for the light mass DM candidate ( $\theta_2 \leq 0.15 \text{ rad}$ ), as investigated in Ref. [19].

Conversely, the contribution from  $\mathcal{H}^\pm$  loop diagrams does not vanish when the masses of heavy up-type quarks are degenerate (*i.e.*,  $\Delta m_{u^H} = 0$ ), but it is enhanced compared with the nondegenerate case, as depicted in the bottom panels of Fig. 5. Furthermore, the contribution is more significant in regions of lighter  $m_{H^\pm}$  and  $m_{u^H}$ . Unlike the  $\mathcal{D}$  loop and  $\mathcal{W}$  loop diagrams, which provide positive contributions to both  $\text{Re}[\Delta C_7]$  and  $\text{Re}[\Delta C_8]$ ,  $\mathcal{H}^\pm$  loop diagrams yield a positive value for  $\text{Re}[\Delta C_7]$  and a negative value for  $\text{Re}[\Delta C_8]$  in the parameter space of interest.

If we also take the up-type SM quark masses (in addition to degenerate up-type hidden heavy quark masses) to be the same, the charged Higgs  $\mathcal{H}^\pm$  loop diagram also vanishes, similar to the SM  $W^\pm$  loop. All these null results for the  $W^\pm$ ,  $\mathcal{W}$ ,  $\mathcal{D}$ , and  $\mathcal{H}^\pm$  loop contributions in the degenerate mass scenarios are simply a manifestation of a generalized version of GIM mechanism [48] in G2HDM<sup>1)</sup>.

Figure 6 presents the real part of  $\Delta C'_7$  and  $\Delta C'_8$ , with the parameter space setup identical to that of Fig. 5. We observe a similar dependence of  $\Delta C'_7$  and  $\Delta C'_8$  on the rel-

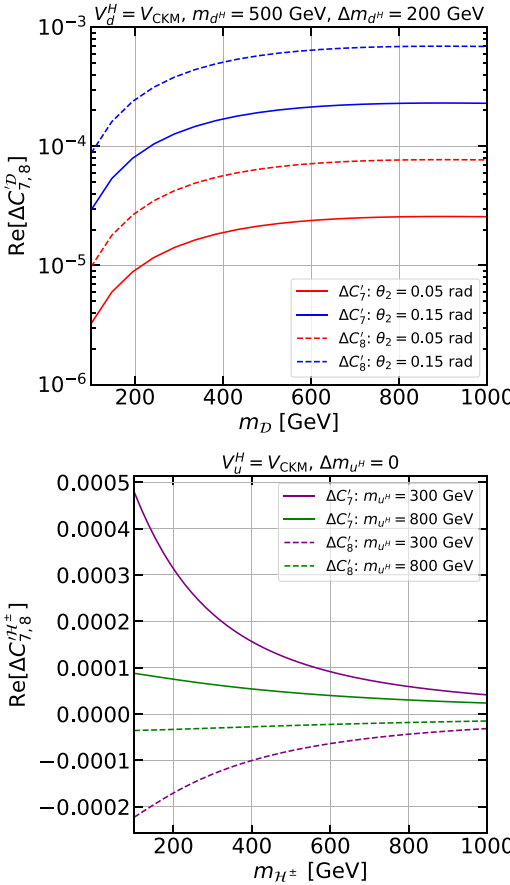


**Fig. 6.** (color online) Similar to Fig. 5 but for  $\Delta C'_7$  and  $\Delta C'_8$ .

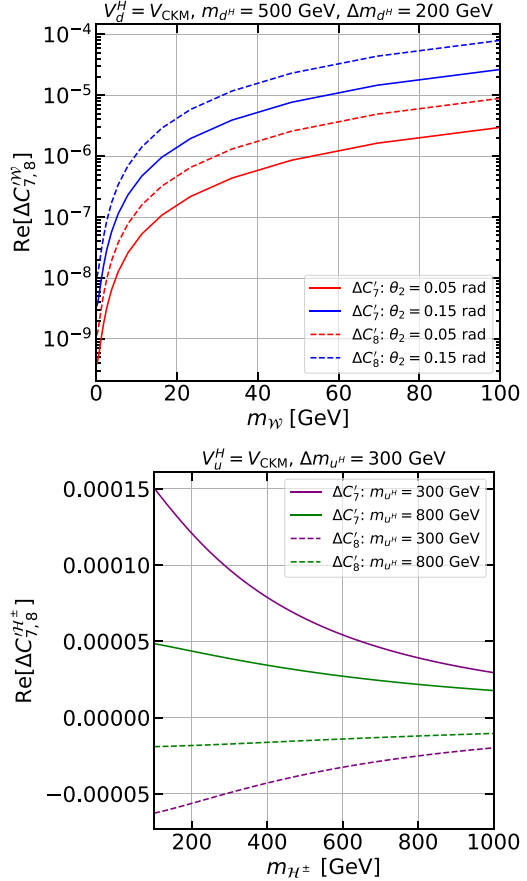
evant parameter space as observed from  $\Delta C_7$  and  $\Delta C_8$ . Moreover, for the  $\mathcal{D}$  loop and  $\mathcal{W}$  loop diagrams,  $\Delta C'_7$  ( $\Delta C'_8$ ) can be approximately two orders of magnitude larger than  $\Delta C_7$  ( $\Delta C_8$ ) within the same parameter space of interest. In contrast, the contribution from the  $\mathcal{H}^\pm$  loop diagrams to  $\Delta C'_7$  ( $\Delta C'_8$ ) is approximately two orders of magnitude smaller than its contribution to  $\Delta C_7$  ( $\Delta C_8$ ).

In Fig. 7, taking the viable data points in the model, we show ratios of the contributions from the  $\mathcal{D}$  and  $\mathcal{W}$  loop diagrams to those from the  $\mathcal{H}^\pm$  loop diagrams in  $|\text{Re}(\Delta C_7)|$  (left panel) and  $|\text{Re}(\Delta C'_7)|$  (right panel). Ultimately, we find that the contribution from  $\mathcal{H}^\pm$  loop diagrams dominates over the  $\mathcal{D}$  loop and  $\mathcal{W}$  loop diagrams.

For comparisons, we also show the leading order (LO) and NLO [51] SM Wilson coefficients  $C_{(7,8)\text{SM}}^{(\ell)}$  at the  $m_W$  scale in Table 1.

## B. Analysis strategy and inputs

In Bayesian analysis, the posterior function is proportional to the product of likelihood function and prior, giving



1) It is well-known that the SM GIM mechanism is not restricted to gauge interactions but also applied to Yukawa interactions with scalar mediators like in MSSM (super-GIM [49]) and mirror fermion model [50].

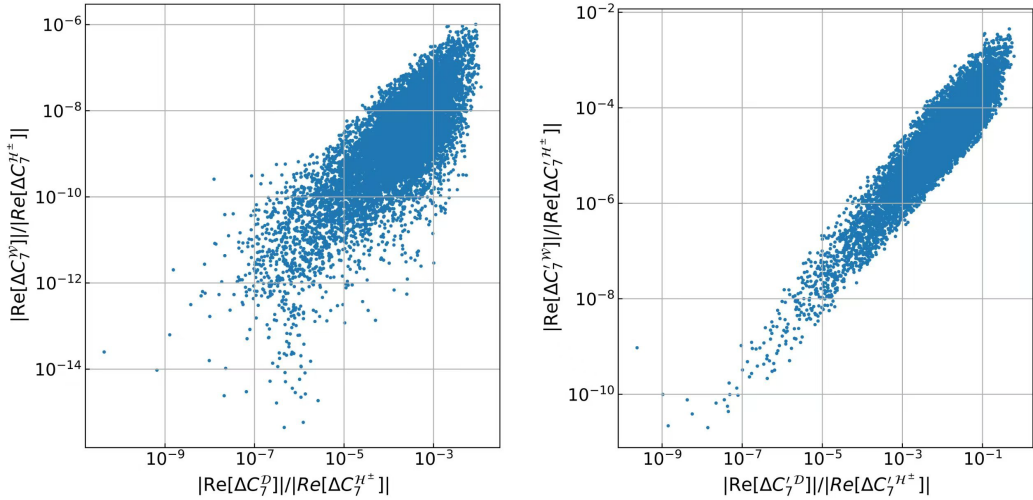


**Fig. 7.** (color online) Ratios of the contributions from the  $\mathcal{D}$  and  $\mathcal{W}$  loop diagrams to those from the  $\mathcal{H}^\pm$  loop diagrams in  $|\text{Re}(\Delta C_7)|$  (left panel) and  $|\text{Re}(\Delta C'_7)|$  (right panel). The scatter points are selected to satisfy the theoretical constraints on the scalar potential [3, 4] and the bounds from oblique parameters [19]. Additionally, we impose  $0 < \theta_2 \leq 0.15$  rad, as required by current constraints for a light-mass dark matter candidate in the model [19].

**Table 1.** LO and NLO SM Wilson coefficients at the  $m_W$  mass scale.

	$C_{7\text{SM}}$	$C_{8\text{SM}}$	$C'_{7\text{SM}}$	$C'_{8\text{SM}}$
LO [51]	-0.1926	-0.0964	-0.0036	-0.0018
NLO [51]	-0.2054	-0.1104	-0.0039	-0.0021

$$\mathcal{P}(\vec{\theta}|O_{\text{expt.}}) \propto \mathcal{L}(O|\vec{\theta})\pi(\vec{\theta}). \quad (45)$$

The negative log likelihood (NLL) function is further defined via  $\chi^2$  as

$$-2\log \mathcal{L}(O|\vec{\theta}) = \chi^2(\vec{\theta}) = (O_{\text{theo.}}(\vec{\theta}) - O_{\text{expt.}})^\top \times (V_{\text{expt.}} + V_{\text{theo.}})^{-1} (O_{\text{theo.}}(\vec{\theta}) - O_{\text{expt.}}), \quad (46)$$

where  $O_{\text{theo.}}$  and  $O_{\text{expt.}}$  denote the theoretical predictions and experimental values, respectively, of observables of interest. Additionally, covariance matrices  $V_{\text{theo.}}$  and  $V_{\text{expt.}}$  incorporate their respective errors <sup>1)</sup>.

The set of observables, including pseudo-observables  $C_8^{(\prime)}(\mu_b)$  <sup>2)</sup>, are summarized as

$$\begin{aligned} O^\top = & [\mathcal{B}(B_s \rightarrow \phi\gamma), \mathcal{B}(B \rightarrow K^{*0}\gamma), \mathcal{B}(B \rightarrow K^{*+}\gamma), \mathcal{B}(B \rightarrow X_s\gamma), \\ & S_{K^*\gamma}, S_{\phi\gamma}, C_{\phi\gamma}, A_{\phi\gamma}^\Delta, C_8, C'_8], \end{aligned} \quad (47)$$

1) The  $V_{\text{expt.}}$  is constructed as a block diagonal matrix using the correlations in experiments, while the  $V_{\text{theo.}}$  is formed as a diagonal matrix assuming they are uncorrelated.

2) Although they are not actual observables, the information extracted from the model-independent global fit [33] is essential for imposing additional constraints on a detailed model.

with the corresponding experimental values collected in **Table 2** and predictions summarized in **Table 3**. For our keen readers, other inputs entered implicitly in the eight observables in (47) to perform the theoretical calculations are summarized in **Table 4**.

### C. Scanning results

To explore the remaining related parameters, we implement the affine-invariant ensemble sampler for Markov chain Monte Carlo (MCMC) [57]. This method enables the posterior function (45) to efficiently converge towards solutions with higher probabilities in the parameter space.

We specify the following priors for the remaining parameters in the model:

$$\vec{\theta} = \begin{cases} m_{d^H} \in [200, 1000] \text{ GeV}, & \Delta m_{d^H} \in [0, 500] \text{ GeV}, \\ m_{u^H} \in [200, 1000] \text{ GeV}, & \Delta m_{u^H} \in [0, 500] \text{ GeV}, \\ m_W \in [0.01, 100] \text{ GeV}, & m_{\mathcal{D}} \in [100, 1000] \text{ GeV}, \\ m_{\mathcal{H}^\pm} \in [100, 1000] \text{ GeV}, & \theta_2 \in [-\frac{\pi}{2}, \frac{\pi}{2}]. \end{cases} \quad (48)$$

These priors assume that each parameter follows a flat prior probability (uniform distribution), which assists in defining the search intervals. The coupling  $g_H$  is related to dark matter mass  $m_W$  and mixing angle  $\theta_2$ , which is explicitly given as

**Table 2.** Experimental values of observables related to  $C_{(7,8)}^{(\prime)}$ .

	$10^5 \mathcal{B}$	$S$	$C$	$A^\Delta$
$B \rightarrow X_s \gamma$	$34.9 \pm 1.9$ [47]	–	–	–
$B_s \rightarrow \phi_s \gamma$	$3.6 \pm 0.5 \pm 0.3 \pm 0.6$ [52]	$0.43 \pm 0.30 \pm 0.11$ [53]	$0.11 \pm 0.29 \pm 0.11$ [53]	$-0.67_{-0.41}^{+0.37} \pm 0.17$ [53]
$B_d^0 \rightarrow K^{*0} \gamma$	$4.5 \pm 0.3 \pm 0.2$ [54]	$-0.16 \pm 0.22$ [47]	–	–
$B_u^+ \rightarrow K^{*+} \gamma$	$5.2 \pm 0.4 \pm 0.3$ [54]	–	–	–

**Table 3.** Predictions of observables related to Table 2.

	$10^5 \mathcal{B}$	$S$	$C$	$A^\Delta$
$B \rightarrow X_s \gamma$	$34.0 \pm 1.7$	–	–	–
$B_s \rightarrow \phi_s \gamma$	$3.35 \pm 0.53$	$0.001 \pm 0.0001$	$0.000 \pm 0.0001$	$0.029 \pm 0.0001$
$B_d^0 \rightarrow K^{*0} \gamma$	$4.15 \pm 0.42$	$0.001 \pm 0.0001$	–	–
$B_u^+ \rightarrow K^{*+} \gamma$	$4.47 \pm 0.45$	–	–	–

**Table 4.** Input parameters adopted in theoretical calculations of observables of interest. In this table, symbols  $\mathcal{Y}_i$  represent the Yukawa couplings, whereas  $y_i$  values are used to correlate measurements with theoretical predictions of  $B_{s,d} \rightarrow V\gamma$  processes.

Parameters	Values	Parameters	Values
$\mathcal{Y}_b/10^{-2}$	1.646(8.2) [55]	$\mathcal{Y}_t$	0.9897(86) [55]
$\mathcal{Y}_c/10^{-3}$	3.646(91) [55]	$\mathcal{Y}_s/10^{-4}$	3.104(36) [55]
$\mathcal{Y}_d/10^{-5}$	1.663(64) [55]	$\mathcal{Y}_u/10^{-6}$	7.80(86) [55]
$m_{B_d}$	5279.72(8) MeV [56]	$m_{B_s}$	5366.93(10) MeV [56]
$m_{B_u}$	5279.41(7) MeV [56]	$m_\phi$	1019.461(16) MeV [56]
$m_{K^{*+}}$	891.67(26) MeV [56]	$m_{K^{*0}}$	895.55(20) MeV [56]
$\tau_{B_s}$	1.520(5) ps [56]	$\tau_{B_u}$	1.638(4) ps [56]
$\tau_{B_d}$	1.517(4) ps [56]	$G_F$	1.1663788(6) $\text{GeV}^{-2}$ [56]
$\alpha_s(m_Z)$	0.1180(9) [56]	$\alpha_e(m_Z)$	1/127.951(9) [56]
$y_s$	0.064(4) [56]	$y_d$	0.0005(50) [56]
$\sin^2 \theta_W$	0.23122(4) [56]	$\phi_s$	-0.010(14) [47]
$\sin \theta_{12}$	0.22501(68) [56]	$\sin \theta_{13}$	0.003732( $^{+90}_{-85}$ ) [56]
$\sin \theta_{23}$	0.04183( $^{+79}_{-69}$ ) [56]	$\delta_{CP}$	1.147(26) [56]

$$g_H = \frac{2m_W}{v} \times \begin{cases} |\sin \theta_2|, & \text{for } \theta_2 > 0, \\ |\cos \theta_2|, & \text{for } \theta_2 \leq 0. \end{cases} \quad (49)$$

Figure 8 shows the favored region from low-energy flavor experiments spanned on sensitive parameters. We found that the dominant contribution to the  $b \rightarrow s\gamma$  process is from charged Higgs diagrams, leading to significant constraints on related parameters such as  $m_{H^\pm}$ ,  $m_{u^H}$ , and  $\Delta m_{u^H}$ , as shown in Fig. 8. In particular, we can place a lower bound on the charged Higgs mass depending on both the hidden up-type quark mass and the mass splitting  $\Delta m_{u^H}$ . Within the  $2\sigma$  confidence interval, we find

$m_{H^\pm} \gtrsim 180$  GeV when  $m_{u^H} \simeq 700$  GeV and  $\Delta m_{u^H} \simeq 350$  GeV. This constraint can become even more stringent in the lower mass range of the hidden up-type quark and for smaller values of the mass splitting <sup>1)</sup>.

In Fig. 9, we present the favored region delineated by low-energy flavor experiments on the  $(m_{H^\pm}, m_{\mathcal{D}})$  plane. Owing to the negligible influence of the  $\mathcal{D}$  diagram, the bounds derived from these experiments exhibit minimal dependence on  $m_{\mathcal{D}}$ . Within the same figure, we also show exclusion regions (purple regions) from theoretical constraints of the scalar potential, which includes the criteria for vacuum stability and perturbative unitarity [3, 4], alongside constraints [19] from oblique parameters [58]<sup>2)</sup>.

1) The bound on the hidden quark mass from direct searches at the LHC are shown in Appendix C.

2) The explicit expressions for the contributions of G2HDM to the oblique parameters  $S$ ,  $T$ , and  $U$  can be found in Ref. [19].

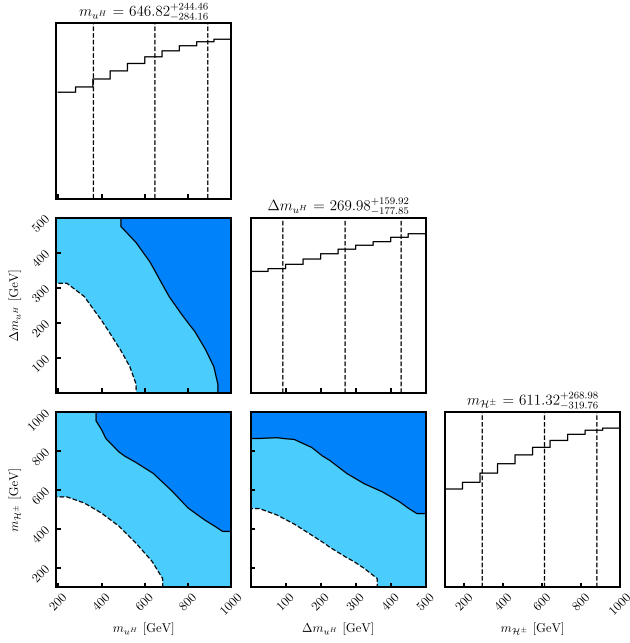


**Fig. 8.** (color online) Parameter space associated with  $\mathcal{H}^\pm$  constrained by low-energy flavor experiments. The solid (dashed) boundary delineates the region of interest, with darker (lighter) shading indicating areas within a 68% (95%) confidence level.

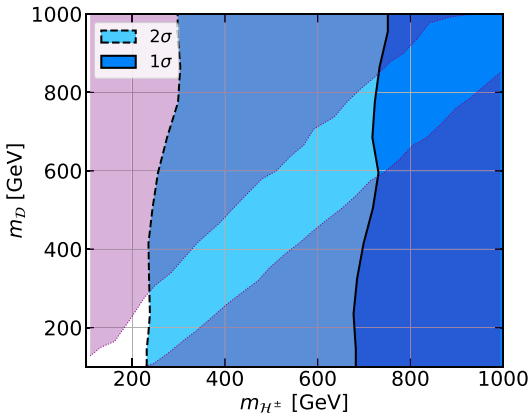


**Fig. 9.** (color online) 68% and 95% confidence level contours from low-energy flavor experiments (lighter blue and darker blue regions), and exclusion regions (purple shaded regions) from a combination of theoretical and oblique parameters constraints projected on the  $(m_{H^\pm}, m_{\mathcal{D}})$  plane.

These constraints introduce a significant correlation between  $m_{H^\pm}$  and  $m_{\mathcal{D}}$ . When these are combined with the low-energy flavor experiment constraints, lower bounds can be established on both  $m_{H^\pm}$  and  $m_{\mathcal{D}}$ . Notably, the regions where  $m_{H^\pm} \lesssim 250$  GeV and  $m_{\mathcal{D}} \lesssim 100$  GeV are excluded at the 95% confidence level through a synergy of constraints from low-energy flavor experiments, oblique parameters, and theoretical constraints imposed on the

scalar potential.

We note that because of the minor contributions from  $\mathcal{D}$  and  $\mathcal{W}$  diagrams, parameters such as  $m_{d^H}$ ,  $\Delta m_{d^H}$ , and  $m_W$  remain relatively unconstrained and are not depicted here.

## VII. CONCLUSIONS

In this study, we have performed computations of the one-loop radiative decay processes for flavor-changing bottom quark transitions  $b \rightarrow s\gamma$  and  $b \rightarrow sg$  within the framework of a minimal G2HDM. Our analysis extends beyond the SM contributions, traditionally mediated by the  $W$  boson, to include one-loop flavor-changing processes in the minimal G2HDM facilitated by new charged current interactions. These interactions are mediated by the dark Higgs ( $\mathcal{D}$ ), charged Higgs ( $\mathcal{H}^\pm$ ), and complex dark gauge boson ( $W^{p,m}$ ), the latter of which is a candidate for dark matter, involving both SM quarks and new heavy quarks in the loops.

We have derived new contributions to Wilson coefficients  $\Delta C_7^{(\prime)}$  and  $\Delta C_8^{(\prime)}$ , with our numerical results shown in Fig. 5 and Fig. 6. Within our parameters of interest, we find that the contributions from  $\mathcal{H}^\pm$  loop diagrams significantly dominate over those from  $\mathcal{D}$  and  $W^{p,m}$  loop diagrams. This dominance is due to the explicit mass factor of SM up-type quarks (primarily top quark) in the Yukawa coupling involving the charged Higgs, SM down-type quarks, and up-type new heavy quarks, as shown in (20), as well as the requirement of mass insertions for internal new heavy quark lines to induce the chirality flipped magnetic and electric dipole operators in (34) and (35). Additionally, the impact of the  $\mathcal{H}^\pm$  loop diagrams is more significant in regions with lighter masses for  $m_{H^\pm}$  and the new heavy up-type quarks.

Interestingly, we observe that the contributions from  $\mathcal{D}$  loop and  $W^{p,m}$  loop diagrams diminish when the masses of the three generations of new heavy quarks running in the loop are degenerate. In contrast, the contributions from  $\mathcal{H}^\pm$  loop diagrams persist under such conditions but also vanish if the masses of the three generations of SM up-type quarks are also set to be degenerate.

Through an exhaustive parameter space scan, constrained by data from various low-energy flavor observables, we have showcased our main results in Fig. 8. Owing to the predominant contribution of the charged Higgs loop diagrams on flavor-changing bottom quark processes, stringent lower bounds have been placed on the masses of the particles involved in the loop, including the charged Higgs and new heavy up-type quarks. Notably, the lower bound on the charged Higgs mass is more restrictive in regions with smaller masses of the new heavy up-type quarks.

By integrating these constraints from low-energy flavor experiments with those from theoretical conditions on

the scalar potential and oblique parameters, we have established lower bounds on the masses of both the charged and dark Higgs. Specifically, regions where  $m_{\mathcal{H}^\pm} \lesssim 250$  GeV and  $m_{\mathcal{D}} \lesssim 100$  GeV are excluded at the 95% confidence level based on our analysis.

Because of the peculiar embedding the two Higgs doublets into a two-dimensional irreducible representation of hidden  $SU(2)_H$  in G2HDM, the Yukawa couplings of charged Higgs are highly correlated with the SM Higgs Yukawa couplings. Thus, flavor physics is quite interesting and rich in G2HDM, as demonstrated in this work for  $b \rightarrow s(\gamma, g)$  in  $B$  physics, as well as in the analogous leptonic process of  $l_i \rightarrow l_j \gamma$  in [32]. Many other low energy flavor physics can be explored further. For instance, new contributions from G2HDM to Wilson coefficients  $\Delta C_9^{(\prime)}$  and  $\Delta C_{10}^{(\prime)}$ , which are relevant to various observables in semileptonic processes such as  $B \rightarrow (X_s, K^{(*)}) l^+ l^-$  and  $B \rightarrow K^{(*)} \nu \bar{\nu}$ , could provide additional insights into NP. Recent global fit studies in LEFT [33] and SMEFT [59] suggest that room remains for NP in these channels. These contributions may play a significant role in further constraining the G2HDM parameter space, potentially providing more stringent limits. Similar considerations apply to  $B$ -meson mixing. Research in this direction is currently in progress and will be reported elsewhere.

## ACKNOWLEDGMENTS

*VQT would like to thank the Medium and High Energy Physics group at the Institute of Physics, Academia Sinica, for their hospitality during the course of this work. TCY and VQT would like to thank Khiem Hong Phan for the hospitality they received at Duy Tân University, HCMC, Việt Nam, where the final phase of this work was completed.*

## APPENDIX A: ONE-LOOP INDUCED AMPLITUDES FOR $b \rightarrow s\gamma$

For the SM  $W$  boson, the unitary gauge has only two diagrams, as depicted in Fig. 1. We obtain

$$A^{(M,E)}(W) = A_1^{(M,E)}(W) + A_2^{(M,E)}(W), \quad (\text{A1})$$

with

$$\begin{aligned} A_1^M(W) = & + \left( \frac{g^2}{8} \right) \sum_j (V_{\text{CKM}})_{j2}^* (V_{\text{CKM}})_{j3} \\ & \times \left[ \mathcal{I}(m_b, m_s, m_{u_j}, m_W) \right. \\ & \left. + \mathcal{I}(m_b, m_s, -m_{u_j}, m_W) \right], \end{aligned} \quad (\text{A2})$$

$$\begin{aligned} A_1^E(W) = & -i \left( \frac{g^2}{8} \right) \sum_j (V_{\text{CKM}})_{j2}^* (V_{\text{CKM}})_{j3} \\ & \times \left[ \mathcal{I}(m_b, -m_s, m_{u_j}, m_W) \right. \\ & \left. + \mathcal{I}(m_b, -m_s, -m_{u_j}, m_W) \right], \end{aligned} \quad (\text{A3})$$

and

$$\begin{aligned} A_2^M(W) = & (-Q_u) \left( \frac{g^2}{8} \right) \sum_j (V_{\text{CKM}})_{j2}^* (V_{\text{CKM}})_{j3} \\ & \times \left[ \mathcal{J}(m_b, m_s, m_{u_j}, m_W) \right. \\ & \left. + \mathcal{J}(m_b, m_s, -m_{u_j}, m_W) \right], \end{aligned} \quad (\text{A4})$$

$$\begin{aligned} A_2^E(W) = & (-i)(-Q_u) \left( \frac{g^2}{8} \right) \sum_j (V_{\text{CKM}})_{j2}^* (V_{\text{CKM}})_{j3} \\ & \times \left[ \mathcal{J}(m_b, -m_s, m_{u_j}, m_W) \right. \\ & \left. + \mathcal{J}(m_b, -m_s, -m_{u_j}, m_W) \right]. \end{aligned} \quad (\text{A5})$$

For the dark Higgs  $\mathcal{D}$  diagram in Fig. 2, we have

$$\begin{aligned} A^M(\mathcal{D}) = & (-Q_d) \left[ \sum_j (S_d^{\mathcal{D}})_{j2}^* (S_d^{\mathcal{D}})_{j3} \mathcal{K}(m_b, m_s, m_{d_j^H}, m_{\mathcal{D}}) \right. \\ & \left. + \sum_j (P_d^{\mathcal{D}})_{j2}^* (P_d^{\mathcal{D}})_{j3} \mathcal{K}(m_b, m_s, -m_{d_j^H}, m_{\mathcal{D}}) \right], \end{aligned} \quad (\text{A6})$$

$$\begin{aligned} A^E(\mathcal{D}) = & i(-Q_d) \left[ \sum_j (P_d^{\mathcal{D}})_{j2}^* (S_d^{\mathcal{D}})_{j3} \mathcal{K}(m_b, -m_s, m_{d_j^H}, m_{\mathcal{D}}) \right. \\ & \left. + \sum_j (S_d^{\mathcal{D}})_{j2}^* (P_d^{\mathcal{D}})_{j3} \mathcal{K}(m_b, -m_s, -m_{d_j^H}, m_{\mathcal{D}}) \right]. \end{aligned} \quad (\text{A7})$$

In the limit where the masses of the three generations of heavy quarks are degenerate, *i.e.*,  $m_{d_1^H} = m_{d_2^H} = m_{d_3^H} = m_{d^H}$ , we obtain

$$\begin{aligned} \sum_j (S_d^{\mathcal{D}})_{j2}^* (S_d^{\mathcal{D}})_{j3} = & \frac{1}{2v^2 v_\Phi^2} [(m_b v_\Phi \cos \theta_2 + m_{d^H} \sin \theta_2) \\ & \times (m_s v_\Phi \cos \theta_2 + m_{d^H} \sin \theta_2)] \\ & \times \sum_j (V_d^H)_{2j} (V_d^H)_{3j}^* = 0, \end{aligned} \quad (\text{A8})$$

$$\begin{aligned} \sum_j (P_d^{\mathcal{D}})_{j2}^* (P_d^{\mathcal{D}})_{j3} &= \frac{1}{2v^2 v_\Phi^2} [(-m_b v_\Phi \cos \theta_2 + m_{d^H} \sin \theta_2) \\ &\quad \times (-m_s v_\Phi \cos \theta_2 + m_{d^H} \sin \theta_2)] \\ &\quad \times \sum_j (V_d^H)_{2j} (V_d^H)_{3j}^* = 0, \end{aligned} \quad (\text{A9})$$

$$\begin{aligned} \sum_j (P_d^{\mathcal{D}})_{j2}^* (S_d^{\mathcal{D}})_{j3} &= \frac{1}{2v^2 v_\Phi^2} [(m_b v_\Phi \cos \theta_2 + m_{d^H} \sin \theta_2) \\ &\quad \times (-m_s v_\Phi \cos \theta_2 + m_{d^H} \sin \theta_2)] \\ &\quad \times \sum_j (V_d^H)_{2j} (V_d^H)_{3j}^* = 0, \end{aligned} \quad (\text{A10})$$

$$\begin{aligned} \sum_j (S_d^{\mathcal{D}})_{j2}^* (P_d^{\mathcal{D}})_{j3} &= \frac{1}{2v^2 v_\Phi^2} [(-m_b v_\Phi \cos \theta_2 + m_{d^H} \sin \theta_2) \\ &\quad \times (m_s v_\Phi \cos \theta_2 + m_{d^H} \sin \theta_2)] \\ &\quad \times \sum_j (V_d^H)_{2j} (V_d^H)_{3j}^* = 0. \end{aligned} \quad (\text{A11})$$

Thus, in this degenerate heavy quark mass limit,  $A^M(\mathcal{D}) = A^E(\mathcal{D}) = 0$ .

For charged Higgs  $\mathcal{H}^\pm$ , from the two diagrams in Fig. 3, we obtain

$$A^{(M,E)}(\mathcal{H}) = A_1^{(M,E)}(\mathcal{H}) + A_2^{(M,E)}(\mathcal{H}), \quad (\text{A12})$$

with

$$\begin{aligned} A_1^M(\mathcal{H}) &= \sum_j (y_u^{\mathcal{H}})_{j2}^* (y_u^{\mathcal{H}})_{j3} \\ &\quad \times [\mathcal{L}(m_b, m_s, m_{u_j^H}, m_{\mathcal{H}}) \\ &\quad + \mathcal{L}(m_b, m_s, -m_{u_j^H}, m_{\mathcal{H}})], \end{aligned} \quad (\text{A13})$$

$$\begin{aligned} A_1^E(\mathcal{H}) &= -i \sum_j (y_u^{\mathcal{H}})_{j2}^* (y_u^{\mathcal{H}})_{j3} \\ &\quad \times [\mathcal{L}(m_b, -m_s, m_{u_j^H}, m_{\mathcal{H}}) \\ &\quad + \mathcal{L}(m_b, -m_s, -m_{u_j^H}, m_{\mathcal{H}})], \end{aligned} \quad (\text{A14})$$

and

$$\begin{aligned} A_2^M(\mathcal{H}) &= (-Q_u) \sum_j (y_u^{\mathcal{H}})_{j2}^* (y_u^{\mathcal{H}})_{j3} \\ &\quad \times [\mathcal{K}(m_b, m_s, m_{u_j^H}, m_{\mathcal{H}}) \\ &\quad + \mathcal{K}(m_b, m_s, -m_{u_j^H}, m_{\mathcal{H}})], \end{aligned} \quad (\text{A15})$$

$$\begin{aligned} A_2^E(\mathcal{H}) &= (-i)(-Q_u) \sum_j (y_u^{\mathcal{H}})_{j2}^* (y_u^{\mathcal{H}})_{j3} \\ &\quad \times [\mathcal{K}(m_b, -m_s, m_{u_j^H}, m_{\mathcal{H}}) \\ &\quad + \mathcal{K}(m_b, -m_s, -m_{u_j^H}, m_{\mathcal{H}})]. \end{aligned} \quad (\text{A16})$$

Unlike the case of the dark Higgs contribution, the charged Higgs contribution does not vanish in the limit where the masses of the heavy quarks running in the loop are degenerate, *i.e.*,  $m_{u_1^H} = m_{u_2^H} = m_{u_3^H} = m_{u^H}$ . However, if we further assume that the up-type SM quarks are also degenerate,  $m_t = m_c = m_u = m_q$ , then

$$\begin{aligned} &\sum_j (y_u^{\mathcal{H}})_{j2}^* (y_u^{\mathcal{H}})_{j3} \\ &= \frac{1}{2v^2} m_q^2 \sum_j (V_u^{H\dagger} V_{\text{CKM}})_{j2}^* (V_u^{H\dagger} V_{\text{CKM}})_{j3} \\ &= \frac{1}{2v^2} m_q^2 (V_{\text{CKM}}^\dagger V_u^H V_u^{H\dagger} V_{\text{CKM}})_{23} \\ &= 0, \end{aligned} \quad (\text{A17})$$

implying that the contribution from the charged Higgs vanishes.

Finally, for the contributions from dark matter gauge boson  $\mathcal{W}$  in the unitary gauge as depicted in Fig. 4, we obtain

$$\begin{aligned} A^M(\mathcal{W}) &= (-Q_d) \left( \frac{g_H^2}{8} \right) \sum_j (V_d^H)_{2j} (V_d^H)_{3j}^* \\ &\quad \times [\mathcal{J}(m_b, m_s, m_{d_j^H}, m_{\mathcal{W}}) \\ &\quad + \mathcal{J}(m_b, m_s, -m_{d_j^H}, m_{\mathcal{W}})], \end{aligned} \quad (\text{A18})$$

$$\begin{aligned} A^E(\mathcal{W}) &= i(-Q_d) \left( \frac{g_H^2}{8} \right) \sum_j (V_d^H)_{2j} (V_d^H)_{3j}^* \\ &\quad \times [\mathcal{J}(m_b, -m_s, m_{d_j^H}, m_{\mathcal{W}}) \\ &\quad + \mathcal{J}(m_b, -m_s, -m_{d_j^H}, m_{\mathcal{W}})]. \end{aligned} \quad (\text{A19})$$

In the limit where  $m_{d_1^H} = m_{d_2^H} = m_{d_3^H} = m_{d^H}$ , Eqs. (A20) and (A21) respectively become

$$\begin{aligned}
A_{deg.}^M(\mathcal{W}) &= (-Q_d) \left( \frac{g_H^2}{8} \right) \left[ \mathcal{J}(m_b, m_s, m_{d^H}, m_W) \right. \\
&\quad \left. + \mathcal{J}(m_b, m_s, -m_{d^H}, m_W) \right] \\
&\quad \times \sum_j (V_d^H)_{2j} (V_d^H)_{3j}^*, \\
&= 0,
\end{aligned} \tag{A20}$$

$$\begin{aligned}
A_{deg.}^E(\mathcal{W}) &= i(-Q_d) \left( \frac{g_H^2}{8} \right) \left[ \mathcal{J}(m_b, -m_s, m_{d^H}, m_W) \right. \\
&\quad \left. + \mathcal{J}(m_b, -m_s, -m_{d^H}, m_W) \right] \\
&\quad \times \sum_j (V_d^H)_{2j} (V_d^H)_{3j}^*, \\
&= 0.
\end{aligned} \tag{A21}$$

In these equations,  $\mathcal{I}$ ,  $\mathcal{J}$ ,  $\mathcal{K}$ , and  $\mathcal{L}$  are the Feynman parametrization loop integrals that can be determined as shown in Appendix B.

## APPENDIX B: FEYNMAN PARAMETRIZATION LOOP INTEGRALS

For convenience, here, we collect loop integrals  $\mathcal{I}$ ,  $\mathcal{J}$ ,  $\mathcal{K}$ , and  $\mathcal{L}$ , which were derived in [32] (See also [60]). Integrals  $\mathcal{I}$  and  $\mathcal{J}$  are entered in the vector gauge boson exchange diagrams, similar to those in Figs. 1 and 4, whereas  $\mathcal{K}$  and  $\mathcal{L}$  are entered in the scalar exchange diagrams, like those in Figs. 2 and 3. We have maintained all the external ( $m_i$  and  $m_j$ ) and internal ( $m_k$  and  $m_X$ ) masses in these integrals. We have checked that if the external masses are small compared with the internal ones, such as in the  $s \rightarrow d$  transition from the  $W$  exchange diagrams, series expansions of expressions of  $\mathcal{I}$  and  $\mathcal{J}$  presented below can be used to reproduce the well-known SM results [61] of heavy quark effects to leading order in  $m_s$  and  $m_d$ .

To avoid word cluttering, we denote  $z \equiv 1 - x - y$  in the following.

### 1. Integrals $\mathcal{I}$ and $\mathcal{J}$

$$\begin{aligned}
\mathcal{I}(m_i, m_j, m_k, m_X) &= \int_0^1 dx \int_0^{1-x} dy \left\{ \frac{1}{-xzm_i^2 - xym_j^2 + xm_k^2 + (1-x)m_X^2} \right. \\
&\quad \times \left[ \left( (y+2z(1-x)) + (z+2y(1-x)) \frac{m_j}{m_i} - 3(1-x) \frac{m_k}{m_i} \right) \right. \\
&\quad \left. \left. + \frac{m_i^2}{m_X^2} x^2 \left( z^2 + y^2 \frac{m_j^3}{m_i^3} + yz \frac{m_j}{m_i} \left( 1 + \frac{m_j}{m_i} \right) - \frac{m_j m_k}{m_i^2} \right) \right] \\
&\quad + \frac{1}{m_X^2} \left( x(1-z) + y + (x(1-y)+z) \frac{m_j}{m_i} - \frac{m_k}{m_i} \right) \\
&\quad + \frac{1}{m_X^2} \left( 2 - x(3-4z) - 3y - z + (2-x(3-4y)-y-3z) \frac{m_j}{m_i} \right) \\
&\quad \left. \times \log \left( \frac{m_X^2}{-xzm_i^2 - xym_j^2 + xm_k^2 + (1-x)m_X^2} \right) \right\}.
\end{aligned} \tag{B1}$$

We note that this integral  $\mathcal{I}$  is for the diagram with two internal charged vector bosons  $X$  coupled to the external photon computed using the unitary gauge. The third line of Eq. (75) is obtained from the product of the transverse pieces of the two vector boson propagators, whereas all the remaining terms are from the product of the transverse and longitudinal pieces of these two propagators. The product of longitudinal pieces do not produce the contributions for the transition magnetic and electric dipole form factors.

$$\begin{aligned}
\mathcal{J}(m_i, m_j, m_k, m_X) &= - \int_0^1 dx \int_0^{1-x} dy \left\{ \frac{1}{-xzm_i^2 - xym_j^2 + (1-x)m_k^2 + xm_X^2} \right. \\
&\quad \times \left[ 2x \left( (1-z) + (1-y) \frac{m_j}{m_i} - 2 \frac{m_k}{m_i} \right) \right. \\
&\quad + \frac{m_i^2}{m_X^2} \left( (1-x) \left( \frac{m_j}{m_i} - \frac{m_k}{m_i} \right) \left( z + y \frac{m_j}{m_i} \right) \left( 1 - \frac{m_k}{m_i} \right) \right. \\
&\quad - z \left( \frac{m_j}{m_i} - \frac{m_k}{m_i} \right) \left( (1-x(1-z)) + xy \frac{m_j^2}{m_i^2} \right) \\
&\quad \left. \left. - y \left( 1 - \frac{m_k}{m_i} \right) \left( xz + (1-x(1-y)) \frac{m_j^2}{m_i^2} \right) \right) \right] \\
&\quad + \frac{1}{m_X^2} \left( y + z \frac{m_j}{m_i} - (1-x) \frac{m_k}{m_i} \right) \\
&\quad + \frac{1}{m_X^2} \left( (1-3y) + (1-3z) \frac{m_j}{m_i} + (1-3x) \frac{m_k}{m_i} \right) \\
&\quad \left. \times \log \left( \frac{m_X^2}{-xzm_i^2 - xym_j^2 + (1-x)m_k^2 + xm_X^2} \right) \right\}.
\end{aligned} \tag{B2}$$

We note that this integral  $\mathcal{J}$  is for the diagram with one internal charged or neutral gauge boson  $X$  exchange, whereas the external photon couples to the internal charged fermion. The diagram is also computed using the unitary gauge. The third line of Eq. (76) is from the transverse piece of the vector boson propagator, whereas the remaining terms are entirely from the longitudinal piece of the propagator.

We can set the final state fermion mass  $m_j = 0$  and consider the limit of either  $m_k \gg m_X, m_i$  or  $m_X \gg m_k, m_i$  for

$\mathcal{I}$  and  $\mathcal{J}$  to deduce

$$\mathcal{I}(m_i, 0, m_k, m_X) \simeq \begin{cases} \frac{1}{6m_X^2} \left( 2 - 3 \frac{m_k}{m_i} \right) + \frac{1}{4m_k^2} \left[ -11 + 18 \frac{m_k}{m_i} + 6 \left( 1 - 2 \frac{m_k}{m_i} \right) \log \left( \frac{m_k^2}{m_X^2} \right) \right] \\ \quad + \frac{m_X^2}{2m_k^4} \left[ -13 + 15 \frac{m_k}{m_i} + 6 \left( 2 - 3 \frac{m_k}{m_i} \right) \log \left( \frac{m_k^2}{m_X^2} \right) \right] + O(m_i, m_X^3), & (m_k \gg m_X, m_i) \\ \frac{5}{6m_X^2} \left( 1 - \frac{12m_k}{5m_i} \right) - \frac{m_k^2}{4m_X^4} + O(m_i, m_k^3), & (m_X \gg m_k, m_i) \end{cases} \quad (\text{B3})$$

$$\mathcal{J}(m_i, 0, m_k, m_X) \simeq \begin{cases} -\frac{5}{12m_X^2} \left( 1 - \frac{6m_k}{5m_i} \right) - \frac{1}{2m_k^2} \left( 1 - 3 \frac{m_k}{m_i} \right) + \frac{m_X^2}{4m_k^4} \left[ -11 + 18 \frac{m_k}{m_i} + 6 \left( 1 - 2 \frac{m_k}{m_i} \right) \log \left( \frac{m_k^2}{m_X^2} \right) \right] \\ \quad + O(m_i, m_X^3), & (m_k \gg m_X, m_i) \\ -\frac{2}{3m_X^2} \left( 1 - 3 \frac{m_k}{m_i} \right) + \frac{m_k^2}{2m_X^4} + O(m_i, m_k^3), & (m_X \gg m_k, m_i) \end{cases} \quad (\text{B4})$$

## 2. Integrals $\mathcal{K}$ and $\mathcal{L}$

$$\mathcal{K}(m_i, m_j, m_k, m_X) = \int_0^1 dx \int_0^{1-x} dy \times \left[ \frac{x \left( y + z \frac{m_j}{m_i} \right) + (1-x) \frac{m_k}{m_i}}{-xym_i^2 - xzm_j^2 + (1-x)m_k^2 + xm_X^2} \right]. \quad (\text{B5})$$

$$\mathcal{L}(m_i, m_j, m_k, m_X) = - \int_0^1 dx \int_0^{1-x} dy \times \left[ \frac{x \left( y + z \frac{m_j}{m_i} + \frac{m_k}{m_i} \right)}{-xym_i^2 - xzm_j^2 + xm_k^2 + (1-x)m_X^2} \right]. \quad (\text{B6})$$

Similarly, we can set the final state fermion mass  $m_j = 0$  and consider the limit of either  $m_k \gg m_X, m_i$  or  $m_X \gg m_k, m_i$  for  $\mathcal{K}$  and  $\mathcal{L}$  to obtain

$$\mathcal{K}(m_i, 0, m_k, m_X) \simeq \begin{cases} \frac{1}{12m_k^2} \left( 1 + 6 \frac{m_k}{m_i} \right) - \frac{1}{6} \frac{m_X^2}{m_k^4} \left( 1 + 3 \frac{m_k}{m_i} \right) + O(m_i, m_X^3), & (m_k \gg m_X, m_i) \\ \frac{1}{6m_X^2} - \frac{m_k}{2m_i m_X^2} \left[ 3 + 2 \log \left( \frac{m_k^2}{m_X^2} \right) \right] \\ \quad + \frac{m_k^2}{12m_X^4} \left[ 11 + 6 \log \left( \frac{m_k^2}{m_X^2} \right) \right] + O(m_i, m_k^3), & (m_X \gg m_k, m_i) \end{cases} \quad (\text{B7})$$

$$\mathcal{L}(m_i, 0, m_k, m_X) \simeq \begin{cases} -\frac{1}{6m_k^2} \left( 1 + 3 \frac{m_k}{m_i} \right) + \frac{m_X^2}{12m_k^4} \left[ -11 - 18 \frac{m_k}{m_i} \right. \\ \quad \left. + 6 \left( 1 + 2 \frac{m_k}{m_i} \right) \log \left( \frac{m_k^2}{m_X^2} \right) \right] + O(m_i, m_X^3), & (m_k \gg m_X, m_i) \\ -\frac{1}{12m_X^2} \left( 1 + 6 \frac{m_k}{m_i} \right) + \frac{m_k^2}{6m_X^4} + O(m_i, m_k^3), & (m_X \gg m_k, m_i) \end{cases} \quad (\text{B8})$$

## APPENDIX C: LHC CONSTRAINTS ON HIDDEN QUARKS

The hidden quarks in our model are color and electric charged particles that can be produced singly or in pairs in a proton-proton collider. Owing to QCD interactions, the production cross section of hidden quarks in such a collider can be significant, similar to squark production in the SUSY model. After production, if kinematically allowed, hidden quarks can decay into a SM quark and a  $h$ -parity odd particle such as  $\mathcal{W}$ ,  $\mathcal{D}$ , or  $\mathcal{H}^\pm$ . If kinematically disallowed or if the decay width is small, the hidden quarks may be stable or metastable. The former scenario results in a jets plus missing transverse energy (MET) signature, whereas the latter leads to a heavy stable charged particles signature. Both signatures have been

searched for at the LHC [62–68], but no significant excess has been observed, thereby setting lower limits on hidden quark mass.

To obtain the LHC limits on hidden quarks in the G2HDM, we use the SModelS v2.3 package [69] interfaced with MicrOMEGAs v6.0 package [70]. Fixing the parameters to  $m_{q^H} = m_{d^H} = m_{u^H}$ ,  $\Delta m_{d^H} = \Delta m_{u^H} = 0$ ,  $m_{H^\pm} = 575$  GeV,  $m_{\mathcal{D}} = 500$  GeV,  $m_{\mathcal{W}} = 1$  GeV, and  $\theta_2 = 0.05$  rad, we find that the most stringent constraint on hidden quark mass is  $m_{q^H} \gtrsim 2.4$  TeV from ATLAS data for jets plus MET searches [63]. Additionally, if assuming the hidden quarks are stable, the CMS data [68] can constrain the hidden quark mass to  $m_{q^H} > 2.15$  TeV. These LHC direct search limits are stronger than those obtained from the  $B$ -physics flavor observable.

## References

- [1] G. Aad *et al.* (ATLAS), *Phys. Lett. B* **716**, 1 (2012), arXiv: 1207.7214[hep-ex]
- [2] S. Chatrchyan *et al.* (CMS), *Phys. Lett. B* **716**, 30 (2012), arXiv: 1207.7235[hep-ex]
- [3] R. Ramos, V. Tran, and T. C. Yuan, *JHEP* **11**, 112 (2021), arXiv: 2109.03185[hep-ph]
- [4] R. Ramos, V. Q. Tran, and T. C. Yuan, *Phys. Rev. D* **103**(7), 075021 (2021), arXiv: 2101.07115[hep-ph]
- [5] W. C. Huang, Y. L. S. Tsai, and T. C. Yuan, *JHEP* **1604**, 019 (2016), arXiv: 1512.00229[hep-ph]
- [6] R. Barbieri, L. J. Hall, and V. S. Rychkov, *Phys. Rev. D* **74**, 015007 (2006), arXiv: 0603188[hep-ph]
- [7] L. L. Honorez, E. Nezri, J. F. Oliver *et al.*, *JCAP* **02**, 028 (2007), arXiv: 0612275[hep-ph]
- [8] A. Arhrib, Y. L. S. Tsai, Q. Yuan and T. C. Yuan, *JCAP* **06**, 030 (2014), arXiv: 1310.0358[hep-ph]
- [9] A. Belyaev, G. Cacciapaglia, I. P. Ivanov *et al.*, *Phys. Rev. D* **97**(3), 035011 (2018), arXiv: 1612.00511[hep-ph]
- [10] Y. L. S. Tsai, V. Tran and C. T. Lu, *JHEP* **06**, 033 (2020), arXiv: 1912.08875[hep-ph]
- [11] Y. Z. Fan, T. P. Tang, Y. L. S. Tsai *et al.*, *Phys. Rev. Lett.* **129**(9), 091802 (2022), arXiv: 2204.03693[hep-ph]
- [12] A. Arhrib, W. C. Huang, R. Ramos *et al.*, *Phys. Rev. D* **98**(9), 095006 (2018), arXiv: 1806.05632[hep-ph]
- [13] C. T. Huang, R. Ramos, V. Q. Tran *et al.*, *JHEP* **1909**, 048 (2019), arXiv: 1905.02396[hep-ph]
- [14] W. C. Huang, Y. L. S. Tsai, and T. C. Yuan, *Nucl. Phys. B* **909**, 122 (2016), arXiv: 1512.07268[hep-ph]
- [15] W. C. Huang, H. Ishida, C. T. Lu *et al.*, *Eur. Phys. J. C* **78**(8), 613 (2018), arXiv: 1708.02355[hep-ph]
- [16] C. R. Chen, Y. X. Lin, V. Q. Tran *et al.*, *Phys. Rev. D* **99**(7), 075027 (2019), arXiv: 1810.04837[hep-ph]
- [17] C. R. Chen, Y. X. Lin, C. S. Nugroho *et al.*, *Phys. Rev. D* **101**(3), 035037 (2020), arXiv: 1910.13138[hep-ph]
- [18] B. Dirgantara and C. S. Nugroho, *Eur. Phys. J. C* **82**(2), 142 (2022), arXiv: 2012.13170[hep-ph]
- [19] V. Tran, T. T. Q. Nguyen, and T. C. Yuan, *Eur. Phys. J. C* **83**(4), 346 (2023), arXiv: 2208.10971[hep-ph]
- [20] A. Arhrib, K. H. Phan, V. Tran *et al.*, *Nucl. Phys. B* **1015**, 116909 (2025), arXiv: 2405.03127[hep-ph]
- [21] M. J. Ramsey-Musolf, V. Q. Tran, and T. C. Yuan, *JHEP* **01**, 129 (2025), arXiv: 2408.05167[hep-ph]
- [22] R. Yang, J. Guo, L. Li *et al.*, *The Line operators in the G2HDM model*, arXiv: 2412.14949 [hep-ph]
- [23] R. N. Mohapatra and G. Senjanovic, *Phys. Rev. Lett.* **44**, 912 (1980)
- [24] G. Senjanovic and R. N. Mohapatra, *Phys. Rev. D* **12**, 1502 (1975)
- [25] S. L. Glashow and S. Weinberg, *Phys. Rev. D* **15**, 1958 (1977)
- [26] A. Crivellin, A. Kokulu and C. Greub, *Phys. Rev. D* **87**(9), 094031 (2013), arXiv: 1303.5877[hep-ph]
- [27] A. Crivellin, D. Müller, and C. Wiegand, *JHEP* **06**, 119 (2019), arXiv: 1903.10440[hep-ph]
- [28] M. Misiak, H. M. Asatrian, K. Bieri *et al.*, *Phys. Rev. Lett.* **98**, 022002 (2007), arXiv: 0609232[hep-ph]
- [29] T. Saito *et al.* (Belle), *Phys. Rev. D* **91**(5), 052004 (2015), arXiv: 1411.7198[hep-ex]
- [30] J. A. Aguilar-Saavedra and B. M. Nobre, *Phys. Lett. B* **553**, 251 (2003), arXiv: 0210360[hep-ph]
- [31] T. T. Q. Nguyen, V. Tran, T. C. Yuan, unpublished
- [32] V. Tran and T. C. Yuan, *JHEP* **02**, 117 (2023), arXiv: 2212.02333[hep-ph]
- [33] Q. Wen and F. Xu, *Phys. Rev. D* **108**(9), 095038 (2023), arXiv: 2305.19038[hep-ph]
- [34] M. Misiak, A. Rehman, and M. Steinhauser, *JHEP* **06**, 175 (2020), arXiv: 2002.01548[hep-ph]
- [35] K. G. Chetyrkin, M. Misiak, and M. Munz, *Phys. Lett. B* **400**, 206 (1997), arXiv: 9612313[hep-ph]
- [36] P. Gambino, M. Gorbahn, and U. Haisch, *Nucl. Phys. B* **673**, 238 (2003), arXiv: 0306079[hep-ph]
- [37] C. Bobeth, P. Gambino, M. Gorbahn *et al.*, *JHEP* **04**, 071 (2004), arXiv: 0312090[hep-ph]
- [38] T. Huber, E. Lunghi, M. Misiak *et al.*, *Nucl. Phys. B* **740**, 105 (2006), arXiv: 0512066[hep-ph]
- [39] M. Czakon, U. Haisch, and M. Misiak, *JHEP* **03**, 008 (2007), arXiv: 0612329[hep-ph]
- [40] A. J. Buras, M. Misiak, M. Munz *et al.*, *Nucl. Phys. B* **424**, 374 (1994), arXiv: 9311345[hep-ph]
- [41] C. Greub, T. Hurth, and D. Wyler, *Phys. Rev. D* **54**, 3350 (1996), arXiv: 9603404[hep-ph]
- [42] L. Everett, G. L. Kane, S. Rigolin *et al.*, *JHEP* **01**, 022

- (2002), arXiv: 0112126[hep-ph]
- [43] H. Eberl, K. Hidaka, E. Ginina *et al.*, Phys. Rev. D **104**(7), 075025 (2021), arXiv: 2106.15228[hep-ph]
- [44] F. Borzumati, C. Greub, T. Hurth *et al.*, Phys. Rev. D **62**, 075005 (2000), arXiv: 9911245[hep-ph]
- [45] A. Paul and D. M. Straub, JHEP **04**, 027 (2017), arXiv: 1608.02556[hep-ph]
- [46] F. Muheim, Y. Xie, and R. Zwicky, Phys. Lett. B **664**, 174 (2008), arXiv: 0802.0876[hep-ph]
- [47] B. Swagato *et al.* (Heavy Flavor Averaging Group), arXiv: 2411.18639 [hep-ex]
- [48] S. L. Glashow, J. Iliopoulos, and L. Maiani, Phys. Rev. D **2**, 1285 (1970)
- [49] S. Dimopoulos and D. W. Sutter, Nucl. Phys. B **452**, 496 (1995), arXiv: 9504415[hep-ph]
- [50] P. Q. Hung, T. Le, V. Q. Tran *et al.*, JHEP **12**, 169 (2015), arXiv: 1508.07016[hep-ph]
- [51] C. Bobeth, M. Misiak, and J. Urban, Nucl. Phys. B **574**, 291 (2000), arXiv: 9910220[hep-ph]
- [52] D. Dutta *et al.* (Belle), Phys. Rev. D **91**(1), 011101 (2015), arXiv: 1411.7771[hep-ex]
- [53] R. Aaij *et al.* (LHCb), Phys. Rev. Lett. **123**(8), 081802 (2019), arXiv: 1905.06284[hep-ex]
- [54] F. Abudinén *et al.* (Belle II), arXiv: 2110.08219[hep-ex]
- [55] T. Deppisch, S. Schacht, and M. Spinrath, JHEP **01**, 005 (2019), arXiv: 1811.02895[hep-ph]
- [56] S. Navas *et al.* (Particle Data Group), Phys. Rev. D **110**(3), 030001 (2024). For the online version, see <https://pdg.lbl.gov/>.
- [57] D. Foreman-Mackey, D. W. Hogg, D. Lang *et al.*, Publ. Astron. Soc. Pac. **125**, 306 (2013), arXiv: 1202.3665[astro-ph.IM]
- [58] M. E. Peskin and T. Takeuchi, Phys. Rev. D **46**, 381 (1992)
- [59] F. Z. Chen, Q. Wen, and F. Xu, Eur. Phys. J. C **84**, 1012 (2024), arXiv: 2401.11552[hep-ph]
- [60] M. Lindner, M. Platscher, and F. S. Queiroz, Phys. Rept. **731**, 1 (2018), arXiv: 1610.06587[hep-ph]
- [61] T. Inami and C. S. Lim, Prog. Theor. Phys. **65**, 297 (1981) [Erratum: Prog. Theor. Phys. **65**, 1772 (1981)]
- [62] M. Aaboud *et al.* (ATLAS), Phys. Rev. D **97**(11), 112001 (2018), arXiv: 1712.02332[hep-ex]
- [63] G. Aad *et al.* (ATLAS), JHEP **02**, 143 (2021), arXiv: 2010.14293[hep-ex]
- [64] A. M. Sirunyan *et al.* (CMS), Phys. Rev. D **96**(3), 032003 (2017), arXiv: 1704.07781[hep-ex]
- [65] A. M. Sirunyan *et al.* (CMS), Eur. Phys. J. C **77**(10), 710 (2017), arXiv: 1705.04650[hep-ex]
- [66] T. Collaboration *et al.* (CMS), JHEP **10**, 244 (2019), arXiv: 1908.04722[hep-ex]
- [67] M. Aaboud *et al.* (ATLAS), Phys. Lett. B **760**, 647 (2016), arXiv: 1606.05129[hep-ex]
- [68] CMS Collaboration, *Search for heavy stable charged particles with  $12.9 \text{ fb}^{-1}$  of 2016 data*, CMS-PAS-EXO-16-036
- [69] M. M. Altakach, S. Kraml, A. Lessa *et al.*, SciPost Phys. **15**(5), 185 (2023), arXiv: 2306.17676[hep-ph]
- [70] G. Alguero, G. Belanger, F. Boudjema *et al.*, Comput. Phys. Commun. **299**, 109133 (2024), arXiv: 2312.14894[hep-ph]